Plant Physiology Preview. Published on October 23, 2017, as DOI:10.1104/pp.17.01401

Short title: **Modeling chlorophyll reduction in soybean canopies**

Corresponding author: **Donald R. Ort**

Full Title: **Chlorophyll can be reduced in crop canopies with little penalty to photosynthesis**

Berkley J. Walker[1,2, 3]
walkerb@uni-duesseldorf.de

Darren T. Drewry[4,5]
ddrewry@jpl.nasa.gov

Rebecca A. Slattery[1,2,6]
rebecca.slattery@ars.usda.gov

Andy VanLoocke[1,7]
andyvanl@iastate.edu

Young B. Cho[1,2]
cho82@illinois.edu

Donald R. Ort[1,2,6]
d-ort@illinois.edu

[1] Global Change and Photosynthesis Research Unit, USDA/ARS, Urbana, IL 61801, USA.
[2] Carl R. Woese Institute for Genomic Biology, University of Illinois, Urbana IL, 61801, USA.
[3] Institute of Plant Biochemistry, Heinrich-Heine University, Düsseldorf, Germany.
[4]Jet Propulsion Laboratory, California Institute of Technology, Pasadena, California, USA.
[5]Joint Institute for Regional Earth System Science and Engineering, University of California, Los Angeles, California, USA
[6] Department of Plant Biology, University of Illinois, Urbana IL, 61801, USA.
[7]Department of Agronomy, Iowa State University, Ames, IA, 50011, USA.

Corresponding author:
Donald R. Ort
Global Change and Photosynthesis Research Unit, USDA/ARS
University of Illinois
1206 W Gregory Dr.
Urbana, IL 61801 USA
d-ort@illinois.edu

One sentence Summary (200 characters)

An empirically parameterized model of canopy photosynthesis in soybeans reveals that leaf chlorophyll can be reduced with significant nitrogen savings and only minor reductions in daily carbon gain.

List of author contributions:

BJW, RAS and DRO conceived the idea of using light-green soybean germplasm to parameterize a canopy model. BJW made the measurements of the light-green soybean optical properties and gas exchange parameters. YBC measured soybean protein content. BJW, DTD and AV designed, performed and interpreted the simulations. BJW, DTD, RAS, AV and DRO wrote the final paper.

Funding information:

This research was supported via subcontract by the Bill and Melinda Gates Foundation (OPP1060461) titled 'RIPE-Realizing Increased Photosynthetic Efficiency for Sustainable Increases in Crop Yield'. D. Drewry was supported by Jet Propulsion Laboratory, California Institute of Technology, under a contract with the National Aeronautics and Space Administration. B. Walker received support from the Alexander von Humboldt Foundation through a postdoctoral fellowship.

Corresponding author email

d-ort@illinois.edu

Abstract:

The hypothesis that reducing chlorophyll content (Chl) can increase canopy photosynthesis in soybeans was tested using an advanced model of canopy photosynthesis. The relationship between leaf Chl, leaf optical properties, and photosynthetic biochemical capacity were measured in 67 soybean accessions showing large variation in leaf Chl. These relationships were integrated into a biophysical model of canopy-scale photosynthesis to simulate the inter-canopy light environment and carbon assimilation capacity of canopies with WT, a Chl-deficient mutant (*Y11y11*), and 67 other mutants spanning the extremes of Chl to quantify the impact of variation in leaf-level Chl on canopy-scale photosynthetic assimilation and identify possible opportunities for improving canopy photosynthesis through Chl reduction. These simulations demonstrate that canopy photosynthesis should not increase with Chl reduction due to increases in leaf reflectance and non-optimal distribution of canopy nitrogen. However, similar rates of canopy photosynthesis can be maintained with a 9% savings in leaf nitrogen resulting from decreased Chl. Additionally, analysis of these simulations indicate that the inability of Chl reductions to increase photosynthesis arises primarily from the connection between Chl and leaf reflectance and secondarily from the mismatch between the vertical distribution of leaf nitrogen and the light absorption profile. These simulations suggest that future work should explore the possibility of using reduced Chl to improve canopy performance by adapting the distribution of the "saved" nitrogen within the canopy to take greater advantage of the more deeply penetrating light.

Abbreviations used

Φ_{CO2}: Quantum efficiency of carbon assimilation (mol CO_2 mol quantum $^{-1}$)

A: Carbon assimilation rates (μmol CO_2 m^{-2} s^{-1})

A_{can}: Canopy carbon assimilation rates (μmol CO_2 m^{-2} ground s^{-1})

A_{leaf}: Leaf carbon assimilation rates (μmol CO_2 m^{-2} s^{-1})

A_n: Net carbon assimilation rates (μmol CO_2 m^{-2} s^{-1})

A-C_i: Photosynthetic response to CO_2 concentration (unitless)

Can_A: Canopy absorbance (unitless)

Can_R : Canopy reflectance (unitless)

Can_T : Canopy transmittance (unitless)

Chl: Chlorophyll content (μmol m^{-2})

DOY: Day Of Year

J_{max}: Maximum rate of electron transport (μmol e m^{-2} s^{-1})

k_n: Coefficient of leaf nitrogen allocation (unitless)

LAD: Leaf Area Density (leaf area/ground area for a given layer volume)

LAI: Leaf Area Index (leaf area/ground area)

L_A: Leaf absorbance (unitless)

L_R : Leaf reflectance (unitless)

L_T: Leaf transmittance (unitless)

MLCan: MultiLayer Canopy-root-soil model

PAR: Photosynthetically Active Radiation (W m^{-2})

PPFD: Photosynthetic Photon Flux Density (μmol m^{-2} s^{-1})

PPFD $_A$: Absorbed Photosynthetic Photon Flux Density (μmol m^{-2} s^{-1})

PSII: Photosystem II

R_d: Leaf day respiration (μmol CO_2 m^{-2} s^{-1})

V_{cmax}: Maximum rate of Rubisco carboxylation (μmol CO_2 m^{-2} s^{-1})

WT: Wild-Type

Introduction

Global food production must increase to provide for the dietary needs of an increasing global population with greater affluence (Ray et al., 2013; Kromdijk and Long, 2016). One strategy to increase food production per unit land area is to increase the efficiency of photosynthetic conversion of Photosynthetic Photon Flux Density (PPFD; units noted in abbreviation table for this and subsequent abbreviations) into biomass, which is currently less than half the theoretical maximum in many major food crops (Long et al., 2015; Ort et al., 2015; Slattery and Ort, 2016). One reason for suboptimal conversion efficiency is that photosynthesis saturates above 25% of full sunlight and most incoming PPFD is absorbed by fully-green upper canopy leaves, meaning that the majority of light absorption occurs where photosynthesis is least efficient due to saturation while lower layers have greater efficiency due to shading (Long et al., 2006; Zhu et al., 2008; Ort et al., 2011; Drewry et al., 2014). This situation suggests that decreasing leaf absorbance (L_A) through reductions in leaf chlorophyll content (Chl) could improve canopy assimilation efficiency by allowing more optimal distribution of PPFD within the canopy.

Increasing canopy photosynthesis through reduced Chl has been considered as a potential optimization strategy for over 30 years (as summarized in Laisk, 1982; Osborne and Raven, 1986). In an early modeling approach integrating the simulated impact of Chl reduction of a single mutant accession to leaf and canopy light distribution to photosynthesis, Chl reduction was projected to increase soybean (*Glycine max* Merr.) canopy photosynthesis by 8% under clear-sky conditions, but much of this gain appears to be due to leaf-level improvements in light-saturated photosynthetic rates (Gutschick, 1984a, 1984b, 1988). Efforts to test the impact of reduced Chl on canopy-level carbon assimilation (A_{can}) have produced conflicting results. While rates of carbon assimilation (A) of mutant algae with reduced light-harvesting capacity often show increased A when grown in mass culture (Melis, 1999; Polle et al., 2003; Mitra and Melis, 2008; Kirst et al., 2012), results from plant canopies are less clear perhaps because they represent complex arrangements of foliage through which radiation transfer

processes and vertical variations in photosynthetic capacity interact (Leuning et al., 1995; De Pury and Farquhar, 1997; Baldocchi et al., 2002).

There is much experimental and computational work examining the possibility of increasing canopy photosynthesis through chlorophyll reduction on plant canopies on soybean (Gutschick, 1984a, 1984b, 1988; Pettigrew et al., 1989; Xu et al., 1994; Drewry et al., 2014; Slattery et al., 2016; Slattery et al., 2017), which grows in dense canopies and has a large variety of accessions with reduced Chl (Supplemental File 1 and Figure 1). One such accession is a magnesium chelatase mutant, *Y11y11* (Campbell et al., 2015), which contains less than half the Chl on a leaf area basis of its nearly isogenic wild type (WT). Some experiments with *Y11y11* show an increase in A_{can} (Pettigrew et al., 1989) and others show little or no effect (Xu et al., 1994; Slattery et al., 2017) despite more even leaf-level light distribution to chloroplasts (Slattery et al., 2016). In the most systematic field examinations to date, leaf rates of carbon assimilation (A_{leaf}), A_{can}, conversion efficiency of absorbed PPFD into biomass, and yield were compared between the *Y11y11* and the nearly isogenic WT. While there were no clear benefits to canopy-level carbon assimilation, there was also little detriment. Despite a >50% reduction in Chl, only modest reductions in biomass and yield were observed likely due to the negative pleiotropic effects specific to *Y11y11* discussed below (Slattery et al., 2017).

126 The conflicting results concerning the benefits of Chl reduction in higher plant canopies
127 may partially result from the limitations of fieldwork where environment is variable and a
128 limited number of accessions can be examined simultaneously. Given the complex interactions
129 of dense plant canopies with incoming PPFD (i.e., Drewry et al, 2010a, Niinemets, 2007;
130 Hikosaka et al., 2016)), it is possible that a selected cultivar with reduced Chl has leaf optical
131 properties that are sub- or supra-optimal for a given season depending on environmental
132 forcing and plant development for that particular year. In addition, negative pleiotropic effects
133 can accompany light-green phenotypes due to the specific nature of the mutation, further
134 confounding experimental results. For example, environmental differences combined with
135 pleiotropic effects might explain the conflicting differences measured in *Y11y11*, which has
136 higher water loss due to increased stomatal conductance. In water replete conditions, *Y11y11*

Figure 1

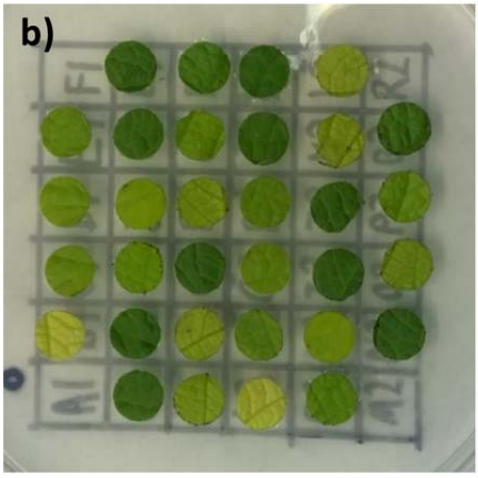

Figure 1: Examples of some of the 67 soybean lines with decreased chlorophyll content (a). Leaf punches prepared for chlorophyll fluorescence imaging (b). Most of the lines were obtained from the USDA soybean germplasm collection and others from the Fast Neutron Soybean Mutagenesis project. Lines were characterized for chlorophyll content, leaf transmittance and leaf reflectance.

had higher A_{can} as compared to WT (Pettigrew et al., 1989), whereas no difference was observed under water-limiting conditions (Slattery et al., 2017).

Since *A* measurements are often localized temporally or spatially to a few positions in the canopy, a vertically-resolved modeling approach that incorporates the detailed biophysical coupling between radiation transfer, photosynthetic biochemical capacity and canopy development can provide insights into the complex relationship between leaf Chl and A_{can}. Here we use a multilayer canopy-root-soil model (MLCan), which couples the biophysical, ecophysiological and biochemical functions of above-ground vegetation with a vertically resolved model of soil moisture to simulate and directly evaluate the impacts of leaf Chl and associated optical properties in canopies that are otherwise identical (Drewry et al., 2010a; Drewry et al., 2010b). MLCan is driven by meteorological data and integrates vertically-resolved leaf-level exchanges of CO_2, water vapor and energy to canopy-scale fluxes. Such canopy

models use assumptions of leaf optical properties (leaf reflectance (L_R); leaf transmittance (L_T); and L_A) to simulate within-canopy distributions of PPFD as functions of downwelling solar radiation, solar zenith angle, foliage density and leaf angle distributions (De Pury and Farquhar, 1997; Campbell and Norman, 1998; Lai et al., 2000; Baldocchi et al., 2002; Drewry et al., 2010a).

An additional consideration of the ability of Chl reduction to increase canopy photosynthesis is the impact of subsequent re-distribution of nitrogen and photosynthetic capacity. Chlorophyll is associated with a large portion of leaf nitrogen, not only present in the Chlorophyll (4 molecules to complex the magnesium ion or 0.06 g N mmol Chl^{-1}), but also in the Photosystem I and II core complexes (PSI and PSII, respectively), and the light harvesting complexes that coordinate the chlorophyll molecules for light energy capture. The chlorophyll binding proteins of the light reactions and antenna complex contain 5,000, 6,040 and 338 mol nitrogen (mol reaction center or LHCII molecule)$^{-1}$ for PSII, PSI and LHCII, respectively (Hikosaka and Terashima, 1995). Assuming that PSII, PSI and LHCII are associated with 60, 184 and 13 chlorophyll molecules each, this means that the total nitrogen associated with each chlorophyll molecule is 1.23, 0.52 and 0.42 g nitrogen mmol Chl^{-1} for chlorophyll associated with PSII, PSI and LHCII respectively (Evans and Seemann, 1989; Kuhlbrandt et al., 1994; Hikosaka and Terashima, 1995; Niinemets and Tenhunen, 1997). In soybean, chlorophyll-related nitrogen is not trivial, for example, fully-expanded field-grown soybean leaves contained 1.75 g nitrogen m^{-2} and Chl of 320 μmol m^{-2} (Ainsworth et al., 2007), resulting in a total chlorophyll-associated nitrogen cost of 8-22% depending on how much chlorophyll is partitioned to each chlorophyll binding protein. This nitrogen must be partitioned through the canopy and theoretical analyses have suggested that the vertical distribution of leaf nitrogen should optimally be in direct proportion to light intensity at a given canopy layer (Field, 1983; Leuning et al., 1995; Sands, 1995), but experimental evidence demonstrates that canopies do not optimally distribute nitrogen, instead over-investing nitrogen when irradiance is low and under-investing when irradiances are high (Niinemets, 2007; Niinemets et al., 2015). These observations suggest two hypothesis that can be tested; 1) There is a significant nitrogen investment in Chl-related proteins that can be decreased through Chl reduction with minimal impact to canopy

177 photosynthesis and 2) Changes in Chl impact canopy PPFD distribution enough to change
178 optimal vertical nitrogen distribution.
179 Here we parameterize MLCan with the field measured relationships among Chl, leaf
180 optical properties, and leaf biochemistry to more realistically simulate the integrated canopy
181 response to Chl reduction, as well as resolve leaf-level variations that could translate to changes
182 in A_{can} and determine the metabolic savings (in terms of actual chlorophyll molecules and
183 associated proteins) of canopies with reduced leaf absorbance (L_A). In one set of simulations,
184 this revised MLCan model was parameterized with leaf properties of a WT (*cv* Clark) and the
185 nearly isogenic low-Chl *Y11y11* mutant (Pettigrew et al., 1989; Campbell et al., 2015; Slattery et
186 al., 2017). In a second set of simulations, we simulated synthetic canopies constructed with
187 foliage across a range of Chl that indicate Chl can be reduced by up to 80% with only slight
188 decreases in A_{can}. Additionally, while Chl reduction can often result in vertically-resolved canopy
189 domains with higher light use efficiencies, these increased efficiencies only resulted in higher
190 net *A* in the lower canopy layers of dense canopies and did not result in a net canopy
191 improvement to carbon fixation capacity. Furthermore, while lower Chl canopies were
192 expected to have different optimal nitrogen distributions, changes in N distribution through the
193 canopy alone were not found to increase A_{can} as compared to dark green canopies. These
194 findings present valuable quantitative relationships between Chl, leaf optical properties and
195 biochemistry for future efforts in optimizing canopy performance through Chl reduction, and
196 more broadly for modeling the impact of Chl variation on canopy biophysics.
197

Results

We present the results of the empirical measurements and numerous canopy simulations in three main sections to better organize their content and motivation. The first section presents the primary empirical relationships among leaf optical properties, photosynthetic biochemistry, and Chl measured across the panel of field-grown soybean accessions displaying a range of Chl that were used to parameterize subsequent canopy simulations in the second and third section. The second section tests if a specific accession (*Y11y11*) is expected to show an increased canopy and/or within-canopy performance through detailed daily and season-long comparisons between a simulated canopy of WT and *Y11y11* soybeans. This accession was selected due to the amount of available field data to provide parameterizations and model validation. The final section determines, by simulating synthetic canopies with a broad range of Chl amounts, if there is any change in leaf Chl level that would be predicted to increase photosynthetic performance. The impact of biochemical capacity scaling with Chl is explored in the simulations of section I and II by either including or not the relationship measured and presented in section I. Additionally, the impact of changing nitrogen distribution, and subsequent vertical biochemical capacity distribution, is investigated in both sets of simulations.

Section I: Empirical relationships among leaf optical properties, photosynthetic biochemistry and Chl

A panel of 67 Chl deficient mutants and parent lines provided an approximately uniform distribution of Chl across the range of ~100 to 500 µmol m^{-2} resulting in a similarly wide range of leaf optical properties (Figure 2). As expected, L_R and L_R decreased with increasing Chl while L_A increased with increasing Chl (Figure 2). Interestingly, although the ratio of L_R to L_R showed no clear trend as a function of Chl (supplemental 1a) the average value across all accessions was ~1 across most of the Photosynthetically Active Radiation (PAR) spectrum (Supplemental 1b). The relationships between Chl and leaf optical properties for the PAR region of the spectrum from the data are shown in Figure 2 (See Equations 1-2 in materials and methods and final fits in Supplemental 3).

Figure 2

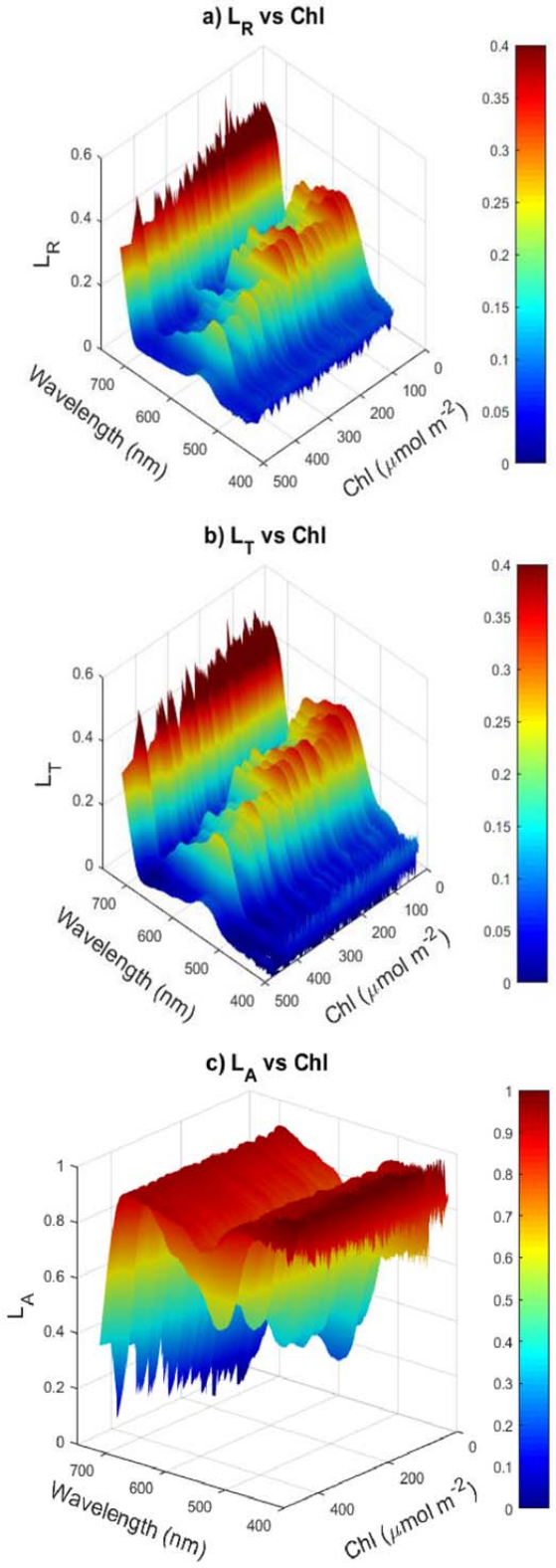

Figure 2: Shown are the relationships between leaf chlorophyll content and reflectance (L_R, a), transmittance (L_T, b) and absorbance (L_A, c) across the spectrum of photosynthetically active radiation.

226 There was a clear relationship between Chl and both V_{cmax} and J_{max} in our accessions

Figure 3

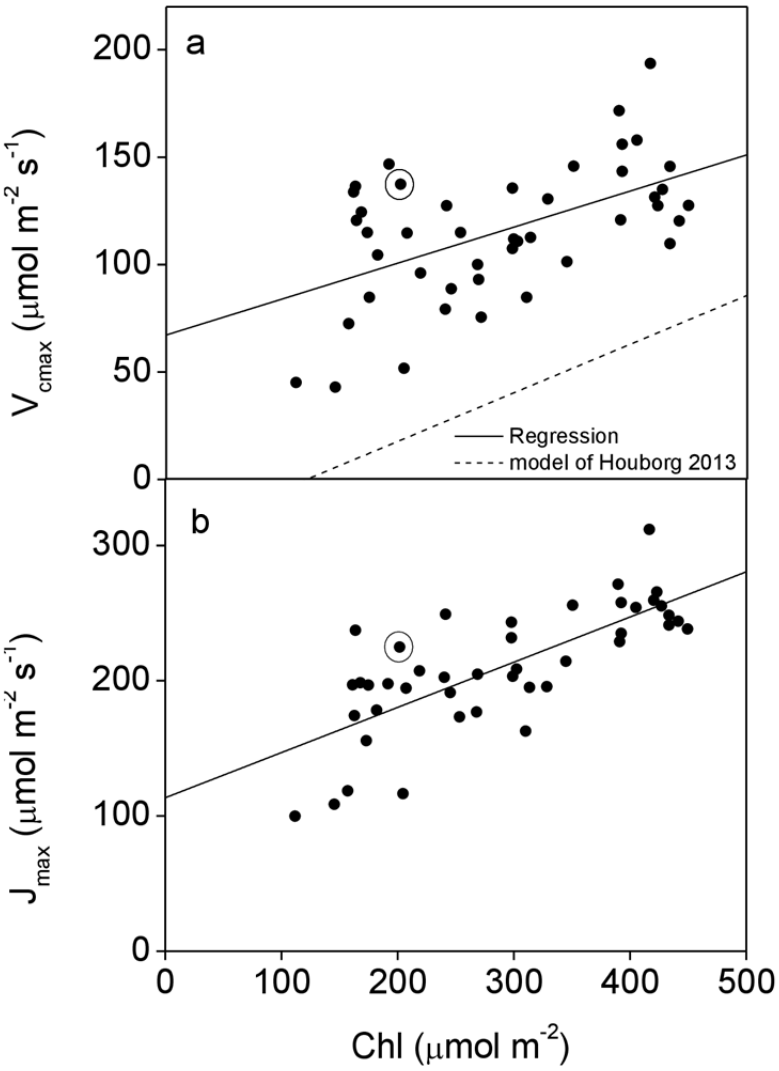

Figure 3: Observed impact of the variation in chlorophyll content (Chl) on photosynthetic performance. 45 plants from various cultivars of soybean were measured using a LI-COR 6400-XT gas exchange system to derive maximum rate of carboxylation (V_{cmax}) and electron transport (J_{max}) from photosynthetic carbon dioxide response curves. Chl was determined from SPAD measurements according to the relationship presented in Supplemental 12. Also shown is the modeled relationship of Chl to V_{cmax} of Houborg 2013 (dotted line). Circled data represents the values measured in the low chlorophyll mutant *Y11y11*.

227 with reduced Chl (Figure 3, Equations 3 and 4 in materials and methods). There was also a
228 strong relationship between Chl and total carotenoids (R^2 = 0.75, Supplemental 2). This
229 relationship was linear for much of the Chl range with between 0.3-0.4 carotenoid molecules
230 per chlorophyll molecule but increased at low Chl until there were more carotenoid molecules
231 than chlorophyll molecules (Supplemental 2b).

Notably, there was variability in the relationship between V_{cmax} and Chl, indicating some cultivars maintained higher V_{cmax} for a given Chl than others and pointing to the potential for the development of plants with low Chl and high photosynthetic biochemical capacity. Consistent with past work, which saw no significant differences in the V_{cmax} or J_{max} of *Y11y11* compared to the WT (Slattery et al., 2017), we saw only slight differences in the V_{cmax} or J_{max} of *Y11y11* as compared to the higher Chl lines (Figure 3). A similar increase in variability across the mean was observed in J_{max} as Chl decreased below ~250 μmol m^{-2} (R^2 of 0.21). This decrease in J_{max} could have been driven in part by lower photosystem II (PSII) quantum efficiency in some mutant lines with reduced Chl. Indeed, chlorophyll fluorescence analysis revealed that the maximum efficiency that PSII was able to use photons to perform photochemistry (F_v/F_m) and electron transport rates (ETR) showed similar increasing variability in these parameters in lines with reduced Chl (Supplemental 4, Baker, 2008). There was no clear correlation between Chl and stomatal conductance (g_s) or leaf day respiration (R_d, Supplemental 5).

Section II: Comparisons between a simulated WT and* Y11y11 *canopy

The relationships measured above were next incorporated into daily and seasonal simulations of WT and *Y11y11* soybean canopies to investigate the PPFD and *A* distribution of this well-studied accession. Seasonal incident PPFD, air temperature, precipitation and ambient water vapor pressure were identical between the WT and *Y11y11* simulations while seasonal variations in leaf area index (LAI) and Chl were constructed from interpolated measurements from the 2013 growing season (Supplemental 6 Slattery et al., 2017). As shown previously, the seasonal LAI was similar between WT and *Y11y11* (Supplemental 6e), but the leaf area distribution (LAD) of *Y11y11* was denser in the lower canopy (Slattery et al., 2017). Leaf optical properties were varied over the growing season according to leaf Chl using the empirically measured relationship for each cultivar (Figure 2, Supplemental 3, equations 1 and 2). Additionally, while not incorporated into MLCan but important for understanding nitrogen use efficiency and partitioning, neither leaf nitrogen nor soluble protein content were different between WT and *Y11y11* for most sampled days, the exception being a significantly higher

soluble protein content on a leaf area and weight basis on DOY 193 (Supplemental 7). Interestingly, since *Y11y11* had about half the Chl as WT and leaf N and soluble protein were similar, this resulted in a lower percentage of leaf nitrogen associated with Chl assuming all Chl was bound by LHCII, the lowest nitrogen containing chlorophyll binding protein (0.42 g nitrogen mmol Chl^{-1}) and a higher protein:Chl ratio in *Y11y11* (Supplemental 7).

Daily simulations of WT and Y11y11 *soybean with accession-specific parameterizations*

To examine the temporally and spatially resolved impacts of variations in chlorophyll content and associated leaf optical properties of field-grown *Y11y11*, simulations were conducted for two representative days of the year (DOY's, 193 and 230) with similar total downwelling PPFD but distinguished by canopy LAI (early and late growing season). These simulations allowed us to visualize the differences in the radiative regime and vegetation function that were induced by the contrasting properties of WT and *Y11y11* plants, both throughout the vertical canopy space and over the course of diurnal variation in environmental forcing (Figure 4). Early in the season when LAI was low (~2.7), WT canopies had only slightly greater PPFD absorbance ($PPFD_A$) than their light green counterparts in the upper ~40% of the canopy, which drove greater *A* at upper layers within the canopy in WT (Figure 4a and c). Later in the season when the canopies were more dense, WT canopies had greater $PPFD_A$ in the upper ~10-20% of the canopy, while *Y11y11* $PPFD_A$ was greater in the lower 75-80% (Figure 4b). These differences in $PPFD_A$ distribution in denser canopies drove different rates of *A* throughout the vertical canopy domain, with WT plants having greater *A* in the top 10% of the canopy at mid-day and *Y11y11* having higher *A* in the lower 90% of the canopy relative to WT plants (Figure 4d). On both days, *Y11y11* canopies generally had a higher quantum efficiency (Φ_{CO2}) in most canopy layers, indicating more efficient use of $PPFD_A$ due to less over saturation of photosynthetic capacity (Figure 4e and f). On DOY 193 the *Y11y11* canopy was more efficient throughout the entire vertical profile for most of the day, excepting short periods at the beginning and end of each photoperiod when oversaturation was low in both canopies due to low incident light levels. On DOY 230 *Y11y11* canopy was more efficient throughout the entire vertical profile for most of the day, except for the bottom 20% of the canopy (Figure 4f).

Figure 4

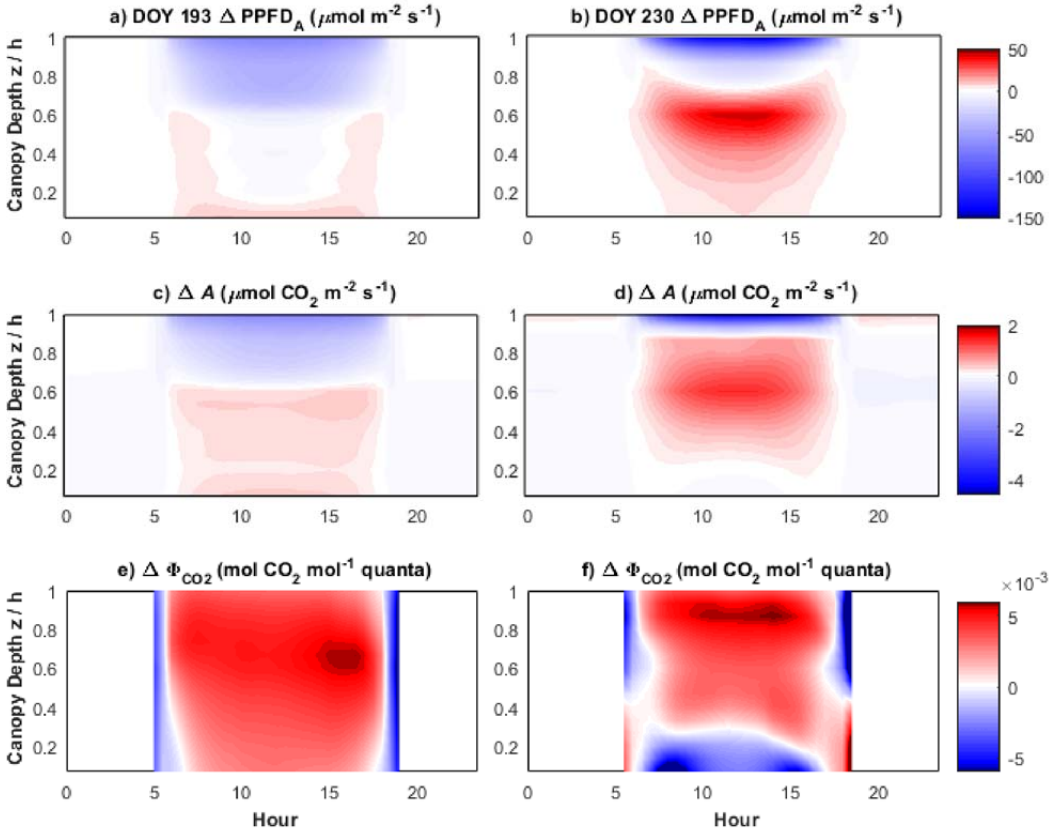

Figure 4: Vertically-resolved, diurnal differences in absorbed PPFD ($\Delta PPFD_A$; a and b), net photosynthetic CO_2 assimilation (ΔA; c and d), and the quantum efficiency of CO_2 assimilation ($\Delta\Phi_{CO2}$; e and f) between a mutant with reduced chlorophyll content (*Y11y11*) and wild-type (WT) before canopy closure early in the growing season (DOY 193 LAI =2.7: a, c and e) and at peak LAI (DOY 230 LAI=7.5: b, d and f). Color maps shows the difference between *Y11y11* and WT canopies (*Y11y11* - WT values) at each of the vertical canopy regions above ground normalized by the canopy height (z/h). Positive values (yellow / red) represent regions of the canopy where *Y11y11* has a larger value than WT, and blue values are regions where the WT values are higher. The two selected days were both cloudless and received similar amounts of total downwelling radiation (Supplemental 5). Wild-type and *Y11y11* canopies were parameterized using genotype-specific chlorophyll contents and leaf area indices (reference Becky's paper here). Values are expressed on a ground area basis.

290

291 *Daily simulations of WT and* Y11y11 *in response to LAI with constant meteorological forcing to*
292 *assess the impact of biochemical scaling with Chl and nitrogen distribution*

293 We next repeated the simulations of Fig. 4 to determine the impact of scaling
294 biochemical capacity with Chl through a canopy with Chl (~50% reduction) similar to *Y11y11*.
295 WT was represented as high Chl=400 µmol m^{-2} and *Y11y11* as low Chl=200 µmol m^{-2} for each of
296 the two assumed LAI's (less dense LAI = 2.7 m^2 m^{-2} and more dense LAI=7.5 m^2 m^{-2}). The
297 simulations using the averaged diurnal cycle of environmental forcing revealed a response

similar to the season-long simulations when photosynthetic biochemical capacity was not scaled with Chl (Supplemental 8). In less dense canopies, high Chl canopies had higher $PPFD_A$ than low Chl canopies at every canopy layer, which in turn drove higher or equal *A* at every canopy layer (Supplemental 8a and c). Interestingly, the higher $PPFD_A$ of high Chl canopies did not drive *A* as efficiently as low Chl canopies, as can be seen from the higher Φ_{CO2} of low Chl canopies at midday throughout much of the canopy profile (Supplemental 8e). In denser canopies, high Chl values produced higher $PPFD_A$ in the upper layers, but not in the lower, resulting in slightly higher *A* in the lower canopy of low Chl canopies, where effective shading by the upper canopy foliage was relatively reduced (Supplemental 8b and d). As expected, the increased light distribution through the canopy resulted in a greater Φ_{CO2} of low Chl canopies through much of the canopy profile (Supplemental 8f). Interestingly, high Chl canopies had a slightly greater Φ_{CO2} in the very lowest regions of the canopy (Supplemental 8f).

However, when photosynthetic biochemical capacity was scaled according to equations 3 and 4, *A* was reduced independently of differences in LAI (Supplemental 9a-d). This resulted in large decreases in Φ_{CO2} in both LAI simulations during the majority of the day when light levels were highest (Supplemental 9e and f). The regions of improved *Y11y11* net carbon exchange forecasted during night-time were a result of decreased modeled R_d, stemming from MLCan's use of V_{cmax} to estimate rates of R_d (*viz*. $R_d = 0.015 * V_{cmax}$).

Seasonal simulations of WT and Y11y11

We next used this approach to examine the dynamics of $PPFD_A$ and *A* throughout the canopy across the entire 2013 growing season using observed forcing data from midday as measured in Champaign, Illinois. Figure 5 shows the differences between WT and *Y11y11* canopies over an almost 90-day period. The same general trends seen in the representative days presented in Figure 4 are seen throughout the growing season. Early and late in the season, there was little difference in $PPFD_A$ or *A* between WT and *Y11y11*, except for slightly larger values for WT plants in the uppermost canopy layers (Figure 5a and c). As canopy density increased between DOYs 200 and 250, $PPFD_A$ and *A* were increased in the uppermost canopy layers of WT relative to *Y11y11*, but the percentage of the vertical profile where *Y11y11* $PPFD_A$ and *A* was greater than WT increased and peaked when LAI was the highest (~DOY 235; Supplemental 6e) during clear-

Figure 5

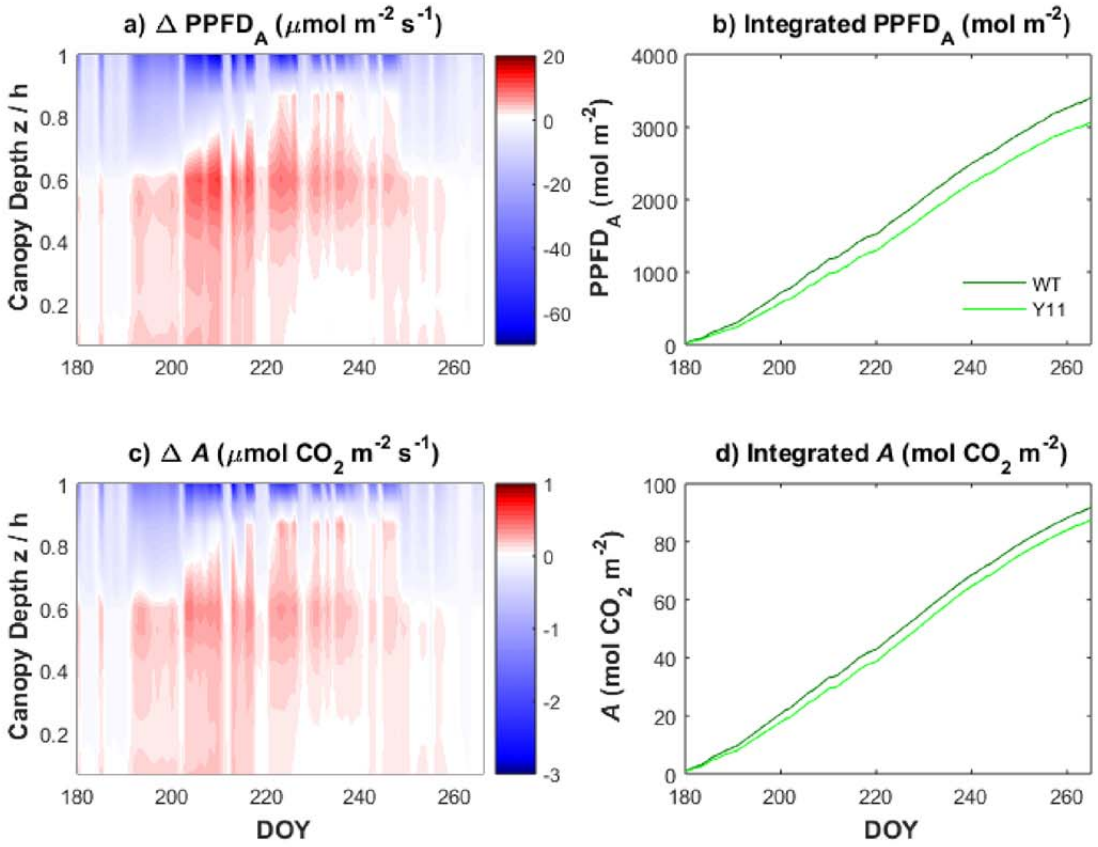

Figure 5: Vertically resolved differences in absorbed photosynthetically active radiation ($\Delta PPFD_A$, a) and net CO_2 assimilation (Δ A, c) between a simulated soybean canopy with reduced chlorophyll content (*Y11y11*) and a wild-type (WT) canopy, at mid-day time points for days of year (DOY) spanning the growing season. Vertical profiles (height above ground normalized by canopy height, z/h) are presented for midday periods (1:00PM) of each day throughout the growing season. Also shown are the seasonally-integrated values for $PPFD_A$ (b) and *A* (d). Color map shows the difference between *Y11y11* and WT canopies (*Y11y11* - WT values) at each of the canopy regions, normalized by the canopy height (z/h). Positive values (more red) represent regions of the canopy where *Y11y11* has a larger value than WT, and more blue values are regions where the WT values are higher. These simulations were driven by field-measured incident radiation, temperatures, and precipitation (see Supplementary Figure 5). Wild-type and *Y11y11* canopies were parameterized using genotype-specific chlorophyll contents and leaf area indices (Slattery 2017).

sky conditions when radiation forcing was greatest. For the daily integrals of $PPFD_A$ and *A* over the duration of the growing season, WT canopies absorbed more PPFD (10%) and assimilated more carbon dioxide (4%) than *Y11y11* (Figure 5ba and d).

The seasonal Φ_{CO2} variations showed that *Y11y11* canopies were more light-use efficient than WT canopies at many canopy layers and on many days during the growing season (Figure 6). With simulations parameterized with *Y11y11*-specific LAI values and using WT biochemical capacity, the vertical profile of Φ_{CO2} agreed with the diurnal profiles from single days, with increased Φ_{CO2} in *Y11y11* simulated at the upper canopy during periods when LAI was the highest (Figure 6a and b, Supplemental 6 and 8). The increased Φ_{CO2} for *Y11y11* in the upper canopy when biochemical parameters were held constant decreased in simulations performed using constant biochemical parameters but LAI and LAD values from WT canopies (Figure 6c). With both assumptions of LAI, Φ_{CO2} appeared at first to increase in *Y11y11* as indicated by the more red regions of the vertical canopy across the season when photosynthetic biochemistry was scaled with Chl (Figure 6b and 6d). While this simulation indicated a higher average Φ_{CO2} value in *Y11y11* with biochemical scaling, a closer examination revealed that the improvements in Φ_{CO2} occurred only when $PPFD_A$ and A_n were the lowest (Supplemental 10).

Section III: Using synthetic canopies to explore a range of Chl and nitrogen distributions

We next used the field data collected across the diverse soybean accessions to develop a second set of simulation experiments designed to quantify canopy performance as a function of leaf Chl. For these simulations of synthetic canopies, the observed LAI values from WT soybeans measured in the 2013 field season were used to allow us to focus on the impacts of varying Chl, photosynthetic biochemical capacity, and canopy nitrogen distribution. Chl was varied across a range representative of the natural variability seen in the experimental population (25-500 $\mu mol\ m^{-2}$).

Impact of assumptions of leaf optical properties to seasonal radiative regimes

Since PPFD reflected from the top of the canopy cannot be used for photosynthesis, the relationship between L_R and L_R with Chl (Figure 2 and Supplemental 2) translates to an increase in PPFD lost due to reflection as Chl decreases. To determine the total impact of increasing PPFD reflectance from the top of the canopy with decreasing Chl on canopy absorbance (Can_A),

Figure 6

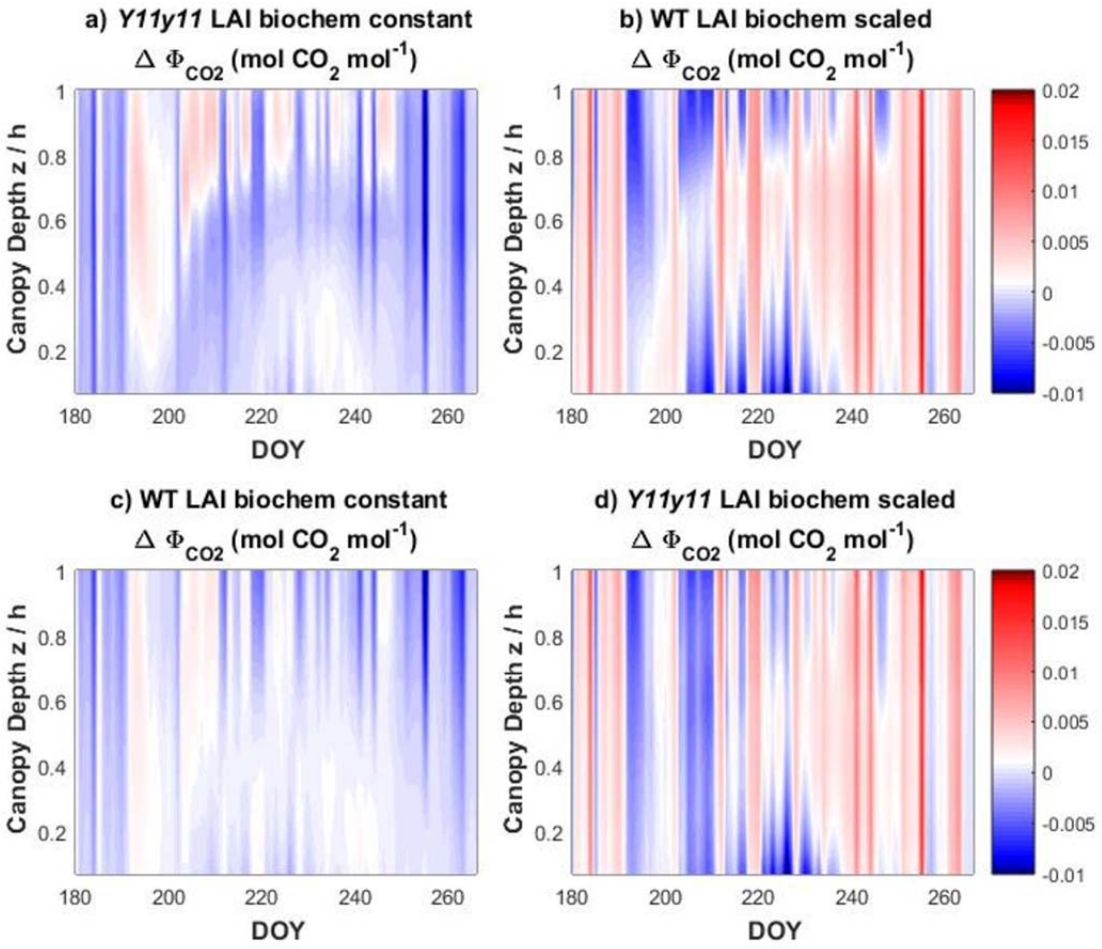

Figure 6: Season long differences in the midday quantum efficiency of CO_2 assimilation ($\Delta\Phi_{CO2}$) between *Y11y11* soybean mutants (*Y11y11*) and wild-type (WT) across the vertical profile of the canopies (height above ground normalized by canopy height, z/h) for the 2013 growing season. Color map shows the difference between *Y11y11* and WT canopies (*Y11y11* - WT) at each of the canopy regions above ground normalized by the canopy height (z/h). Positive values (more red) represent regions of the canopy where *Y11y11* has a larger value than WT, and more blue values are regions where the WT values are higher. Simulations were performed assuming the genotype-specific chlorophyll content (Chl) and *Y11y11* values for leaf area index (LAI) and constant photosynthetic biochemical capacity (V_{cmax} and J_{max}; a), WT LAI and biochemical capacity scaled with Chl (b), WT LAI and a constant photosynthetic biochemical capacity (c) and *Y11y11* values for LAI and biochemical capacity scaled with Chl (d). Environmental forcing (precipitation, downwelling radiation, temperature, H_2O vapor pressure and wind speed) for the simulations were taken from the 2013 growing-season.

we simulated two distinct scenarios. In the first scenario (Figure 7 a,c,e), we scaled L_R with Chl according to Equation 2. In the second scenario (Figure 7 b,d,f), we maintained L_R at a negligible

Figure 7

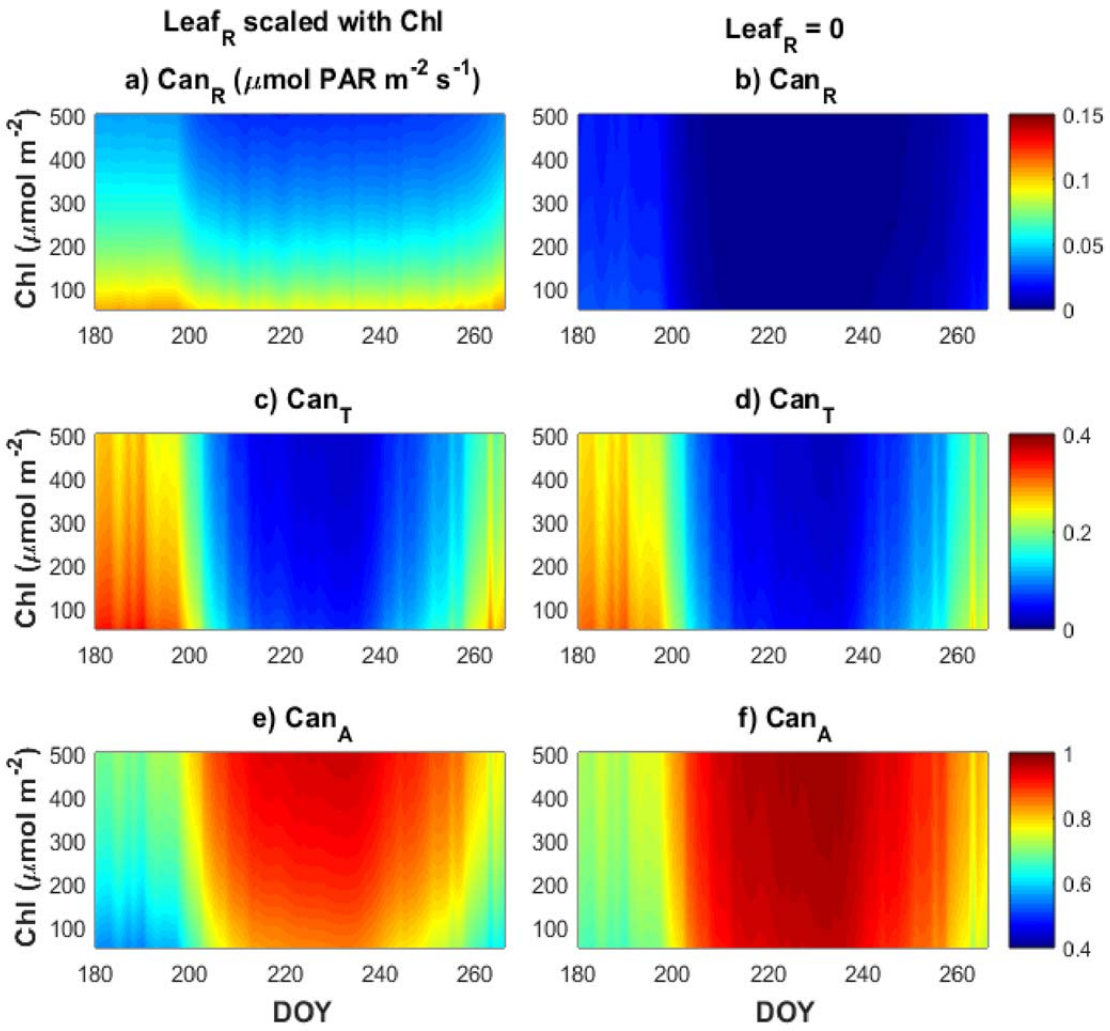

Figure 7**:** Total canopy reflectance (Can_R; a and b), transmittance (Can_T; c and d) and absorbance (Can_A; e and f) in simulated canopies composed of a range of leaf chlorophyll contents (Chl) going from dark green (500 μmol m^{-2}) to light green (50 μmol m^{-2}) according to DOY within the growing season. Total values for each optical property were determined by summing the diurnal values for PPFD reflected, transmitted or absorbed by the canopy divided by the summed total of diurnal incoming PPFD. Simulations were performed assuming leaf reflectance ($Leaf_R$)and transmittance ($Leaf_T$) co-varied according to empirical relationships (a, c, e; Equation 1 and 2) derived from observations of diverse soybean lines (see Figure 2) spanning a wide range of Chl as indicated by the decreasing Chl displayed on the y-axis. Alternatively, canopies were simulated with $Leaf_R$ set to a negligible value at every Chl (b, d and f) to show the impact of leaf reflective loss on total canopy optical properties.

361 value. L_R was always assumed to scale with Chl according to equation 1. Canopy optical

362 properties were closely related to the leaf optical properties applied throughout the canopy, as

well as total canopy LAI. Canopies with higher leaf Chl showed corresponding decreases in canopy transmittance (Can_T) and reflectance (Can_R, Figure 7a, c and e). Seasonal variations in LAI drove additional interactions, with the peak of the growing season resulting in significantly decreased Can_R and Can_T, as most PPFD was absorbed by the vegetation across all Chl levels for the canopy densities examined here. When L_R was modeled as negligible to assess the impact of increased albedo loss to Can_A in canopies with reduced Chl, there was very little Can_R compared to canopies with L_R scaled according to Equation 2 (Figure 7a and b). The small amount of Can_R early and late season arose from the soil reflectance when the canopy was least dense. Decreased Can_R translated to increased Can_A in canopies with negligible L_R, especially when Chl was low (Figure 7e and d). Since these simulations characterize only the light environment of the canopy, they were not sensitive to different assumptions of photosynthetic capacity distribution or sensitivity to Chl.

Impact of Chl reduction to seasonal canopy photosynthesis

We next examined the impact of Chl variation on A_{can} and Φ_{CO2} with various assumptions of L_R Chl response and biochemical sensitivity (Figure 8). Reductions in Chl decreased A_{can} under all simulated conditions except for when L_R was kept at a negligible value and biochemistry was not scaled with Chl, where A_{can} increased by a maximal ~2% when Chl was 75 μmol m^{-2} (Figure 8a, Supplemental 10). When photosynthetic capacity was held constant but L_R scaled with Chl, noticeable reductions occurred in A_{can} below 275 μmol m^{-2} (Figure 8a). When leaf photosynthetic biochemical capacity was varied with Chl according to our empirical relationships, canopy performance was highly sensitive to Chl with a steep decrease in A_{can} along the simulated Chl gradient (Figure 8a). Φ_{CO2} increased when photosynthetic biochemical capacity was held constant (Figure 8b, Supplemental 10). In contrast, Φ_{CO2} generally decreased when leaf photosynthetic biochemical capacity decreased with Chl.

Combined impact of leaf optics and nitrogen distribution on canopy photosynthesis for a representative day

Figure 8

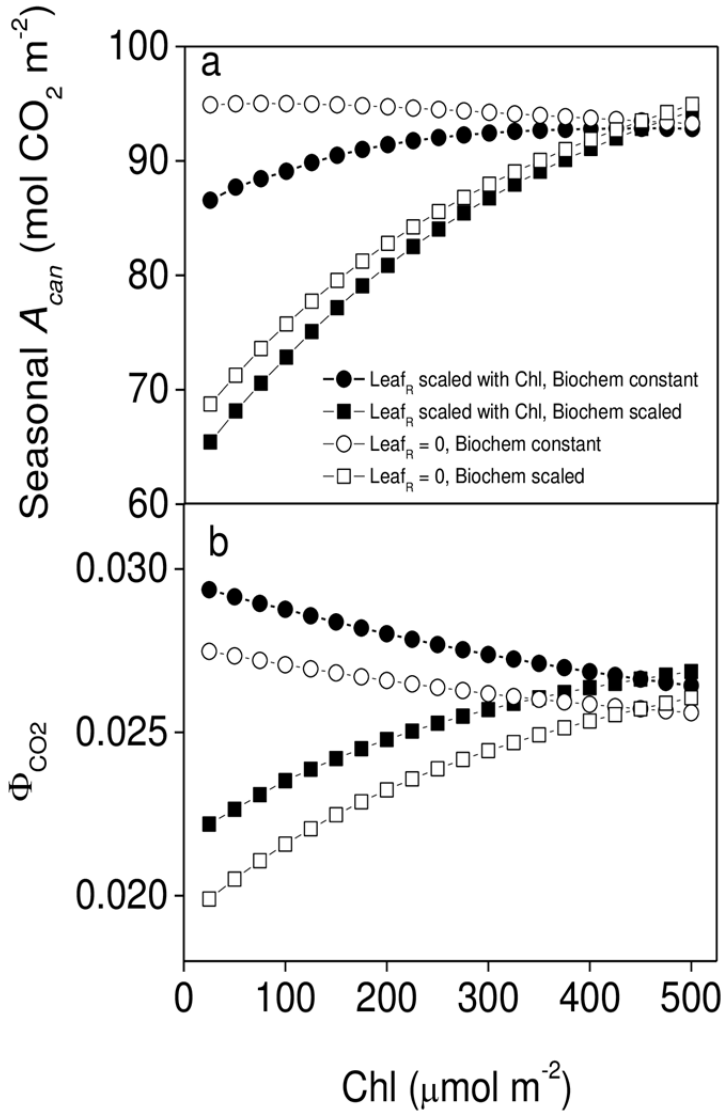

Figure 8 Impact of chlorophyll content (Chl) reduction on the seasonal simulated soybean photosynthesis (A_{can}; a) and the quantum efficiency of CO_2 fixation (Φ_{CO2}; b). Seasonal values are shown for the 2013 growing season (see Supplemental Figure 5). Simulations were performed assuming leaf photosynthetic biochemical capacity remained constant despite chlorophyll content (Chl; circles) or that it scaled with Chl according to Equations 3 and 4 (squares). Leaf reflectance and transmittance were also assumed to both vary with Chl according to Equations 1 and 2 (filled symbols) or leaf reflectance remained constant despite changes in Chl (open symbols) to determine the impact of changes in reflective loss on canopy performance.

391 In MLCan, the vertical distribution of photosynthetic capacity is scaled with nitrogen

assuming an exponential decay function containing k_n in the exponent (See Materials and Methods, De Pury and Farquhar, 1997). To determine if the greater Φ_{CO2} and PPFD penetration in the low Chl canopies could result in improved A_{can} by distributing biochemical capacity deeper into these regions, we next ran one-day simulations where Chl and nitrogen distribution were varied combinatorially. To modify nitrogen distribution, we used different values of the exponential decay term k_n (set as 0.5 as a default and in previous simulations) to determine the impact on canopy PPFD absorbance and performance among three different Chl contents (Supplemental 12). In these simulations the nitrogen distributions of different k_n assumptions were scaled so that total canopy nitrogen was not varied with k_n (see Materials and Methods). Higher k_n resulted in nitrogen more quickly decreasing with depth in the canopy (Supplemental 12). Additionally, decreased leaf Chl increased the proportion of PPFD absorbed in the lower canopy in the three Chl values shown (400, 200 and 50 μmol m^{-2}). There was good agreement between the nitrogen distribution and PPFD absorbance profiles at k_n values between 0.3 and 0.5 when Chl = 400 and 200 μmol m^{-2}, while at the lowest Chl of 50 μmol m^{-2} the best agreement was observed at k_n values slightly less than 0.3. This suggests that the optimal nitrogen distribution, represented by k_n, should be somewhat sensitive to Chl.

To determine the combinatorial effect of nitrogen distribution and Chl to A_{can}, we performed daily simulations of A_{can} parameterized with different assumptions of A_{can} and k_n under average field data weather forcing and LAI = 7.5 m^2 m^{-2}(Figure 9). These simulations confirmed that the k_n value that produces the highest A_{can} changes with Chl, as can be seen by the shifting regions of highest A_{can} as Chl decreased under both assumptions of L_R (Figure 9). When L_R was scaled with Chl, the optimal k_n shifted from ~0.45 at 500 μmol $m^{-2}$to ~0.35 at the lowest Chl values (Figure 9a), in agreement with the values of k_n that produced nitrogen profiles in the closest agreement with $PPFD_A$ profiles (Supplemental 12). In all cases when L_R was scaled with Chl, A_{can} decreased with Chl, regardless of k_n (Figure 9a). Consistent with the seasonal simulations (Figure 8), A_{can} increased with reduced Chl when L_R was set to a negligible value (Figure 9b). Interestingly, the increase in A_{can} was dependent on k_n, further demonstrating that L_R and nitrogen distribution conspire to impair the ability of Chl reductions to increase A_{can}.

Figure 9

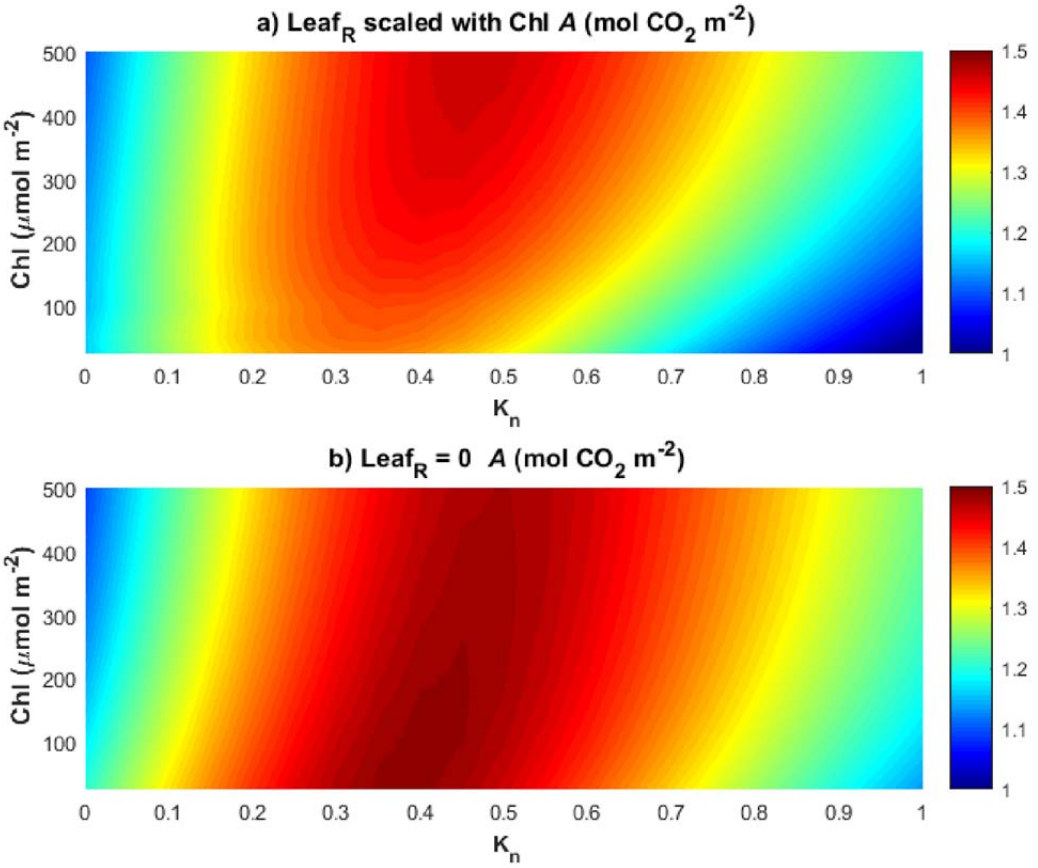

Figure 9: The response of total daily canopy carbon assimilation (A_{can}) to different assumptions of chlorophyll content (Chl) and canopy nitrogen distribution profiles. Canopy nitrogen profiles were adjusted through varying k_n, a term describing the exponential decay of nitrogen through a canopy profile (See Supplemental 7 and Materials and Methods for more detail). Environmental forcing (radiation, temperature, relative humidity...etc) was taken as the average daily conditions for the 2013 growing season. Shown are the relationships between Chl, nitrogen distribution and canopy A assuming leaf reflectance ($Leaf_R$)and transmittance ($Leaf_T$) co-varied according to empirical relationships (a) and assuming $Leaf_R$ was negligible (b).

Discussion

Chl reduction alone does not directly improve canopy photosynthesis

Our findings predict that reductions in Chl are not expected to increase A_{can} by increasing light penetration into soybean canopies when the canopy is examined as a whole under realistic modeling assumptions (Figure 8, Supplemental 10). However, a light-green canopy can have

regions of greater $PPFD_A$ and *A*, resulting in increased Φ_{CO2} through much of the vertical canopy domain of light-green mutants (Figure 4-6, Supplemental 8). For the simulations conducted here, the gains in Φ_{CO2} in the lower light-green canopy were not enough to offset the higher *A* of upper-canopy foliage in dark green canopies. The increase in *A* found in the lower regions of the light-green canopy during the part of the growing season with peak LAI and greatest incident PPFD (Figures 4 and 5) indicates that improvements to total light-green canopy performance could be realized if biochemical capacity were redistributed to better take advantage of redistributed PPFD (discussed further below). Our findings also indicate that Chl can be drastically reduced with little impact to A_{can}, suggesting an over-investment in Chl and an under-utilization of photosynthetic biochemical capacity in much of the canopy space of modern soybean cultivars.

Nitrogen distribution and the future of light-green canopies

The inability of light-green canopies to achieve increased A_{can}, despite increases in $PPFD_A$ and *A* in the lower canopy, partially results from the way photosynthetic biochemical capacity is distributed spatially through the canopy (Figure 9 and Supplemental 12). MLCan is coded to decrease photosynthetic biochemical capacity exponentially with canopy depth, according to the decay of nitrogen content found in a variety of crops and herbaceous plants including >16 cultivars of wheat, *Vicia faba*, *Oryza sativa*, *Glycine max*, *Sorghum bicolor, Amaranthus cruentus*, *Helianthus annuus*, *Hibiscus cannabinus*, *Cynara cardunculus,* and *Carex acutiformis* (Schieving et al., 1992; Anten et al., 1995; Anten, 1997; De Pury and Farquhar, 1997; Del Pozo and Dennett, 1999; Dreccer et al., 2000; Yin et al., 2003; Archontoulis et al., 2011; Moreau et al., 2012). Because of the lack of re-partitioning the nitrogen profile in the simulations, the relative increase in availability of PPFD over the majority of the vertical canopy space in the low Chl canopy (Figures 4 and 5) did not result in higher A_{can} partially since photosynthetic biochemical capacity was not re-partitioned spatially to regions where the light green canopy was most efficient, such as in the deepest canopy regions (Figure 9). For example, on DOY 230 the lower 20% of the canopy absorbed more PPFD (Figure 4b) but had a lower *A* (Figure 4d) resulting in a lower Φ_{CO2} (Figure 4f).

455 The optimal re-adjustment in nitrogen distribution would need to vary temporally (or
456 with LAI) as illustrated from the differences in the example DOYs of Figure 4 to take best
457 advantage of the re-distributed PPFD in light green canopies. Similarly, the simulations also
458 revealed A_{can} did not increase with Chl reduction despite many combinations of Chl and k_n
459 (Figure 9a). It has also been proposed that a nitrogen re-allocation within photosynthetic
460 capacity has the potential to improve *A* within a single leaf in future climates based on
461 modeling of optimal partitioning of V_{cmax} and J_{max} under future climate scenarios (Kromdijk and
462 Long, 2016). The use of k_n to represent nitrogen distribution has not been conclusively linked to
463 biological constraints, suggesting that other distributions are possible. Future work could
464 explore direct optimizations of nitrogen distribution in the canopy with validation work in field-
465 grown canopies to determine if more complex nitrogen distribution strategies could take better
466 advantage of re-distributed PPFD under current and future climates.
467 While these simulations and field data do not support that Chl reductions would result
468 in higher *A* through more optimal light distribution when implemented alone or even with re-
469 distributions of nitrogen across the canopy profile, they do indicate that a canopy can
470 accommodate drastic reductions of Chl (as low as 16% of WT), with only minimal impacts on
471 A_{can}. If a plant could have similar *A* with less investment in nitrogen associated with Chl (both
472 directly in Chl and in Chl-associated protein complexes), this would free-up nitrogen to be re-
473 mobilized from antennae complexes to more limiting processes within the leaf. Indeed, leaf
474 nitrogen seems to be conserved despite the reduced Chl of *Y11y11* (Supplemental 7) meaning
475 that nitrogen assimilation and uptake in soybean is not sensitive to the demand based on
476 chlorophyll biosynthesis. While it is not clear where nitrogen is diverted to in reduced Chl
477 mutants, this nitrogen could have substantial benefits if re-invested into photosynthesis,
478 especially since many of the enzymes involved in carbon metabolism appear to have limiting
479 sub-optimal activities (Zhu et al., 2007). For example, a reduction of Chl from 500 to 100 µmol
480 m^{-2} would result in a savings of 400 µmol m^{-2}, which translates to a nitrogen savings of 0.17 g
481 nitrogen m^{-2}, assuming all the reduced Chl was bound to the light harvesting complex for
482 photosystem II, the lowest nitrogen containing chlorophyll binding protein (0.42 g nitrogen
483 mmol Chl^{-1}). This is would represent an 8-12% savings in total leaf nitrogen assuming the WT

leaf nitrogen contents we measured during the field season (Supplemental 7). Such nitrogen savings could have a sizable positive impact on yield, since even nitrogen-fixing *G. max* is often nitrogen limited (Salvagiotti et al., 2008). It is interesting that in *Y11y11*, the nitrogen saved from reduced Chl investment is still maintained by the leaf as evidenced by the identical nitrogen and protein contents of both genotypes for all but one sampling day (Supplemental 7), raising the question of where nitrogen is mobilized in reduced Chl plants if not to photosynthesis.

The positive impact of redirecting nitrogen from Chl to limiting enzymes in photosynthesis was recently demonstrated in a simulated rice canopy using a ray-tracing algorithm coupled to a complete biochemical representation of C_3 photosynthesis (Song et al., Accepted). In this model, there was only a modest benefit of reducing Chl content alone (~3% increase in A_{can}), but when the saved nitrogen was re-invested in limiting enzymatic steps of C_3 photosynthesis, both A_{can} and nitrogen use efficiency could be increased by 30%. The next logical step for canopy optimization through canopy Chl reduction is therefore to understand where nitrogen is partitioned in plants with reduced Chl and how this repartitioning can be more optimally engineered. In addition to the coupled ray-tracing and C3 metabolic model of Song *et al.*, there are additional frameworks for repartitioning nitrogen based on five competing photosynthetic sinks using a co-limiting model parameterized by empirically-derived relationships (Hikosaka and Terashima, 1995). This particular model, however, is not compatible with MLCan since MLCan uses the mechanistic biochemical relationships of photosynthesis to simulate canopy response to radiation and atmospheric conditions. The relationship between Chl and V_{cmax} and J_{max} indicate that nitrogen re-allocation from antenna complexes to photosynthetic biochemical capacity does not happen generally as a result of mutations that reduce Chl (discussed further below), but it is possible that more targeted engineering strategies could help achieve this goal.

Trade-offs between leaf reflectance and transmittance limit the benefits of light green canopies

The inability of Chl reductions to increase canopy light penetration enough to increase *A* also partially results from the observed relationship between L_R and L_R (**Error! Reference source not**

found. and Supplemental 2). Both L_R and L_R increase with decreasing Chl since both originate from the scattering of light within the complex inner anatomy of the leaf due to the differences in the refractive indices between air (1.00) and cell material (~1.48, Woolley, 1971). Thus L_R and L_R only differ in the direction of the light scattering and result from the many air-to-cell interfaces within a leaf (Woolley, 1971; Terashima and Saeki, 1983), a relationship confirmed in our observations (Figure 2 and Supplemental 3). The largest amount of reflected PPFD occurs from the upper canopy layer, where incident radiation is greatest. Reflected PPFD from the upper canopy is lost from the canopy and not available to drive *A*, resulting in decreased Can_A (Figure 7e). The decrease in Can_A is not fully compensated for by increases in Φ_{CO2} when L_R and L_R are set equal to the relationships in equation 1 and 2 (Figure 8b), resulting in decreased *A* in lower Chl canopies (Figure 8a). Only when L_R is reduced to a negligible value do simulated reduced Chl canopies have greater A_{can} (Figures 8a and 9b), demonstrating that the increased reflective loss of PPFD from the leaf surface accompanying Chl reduction partially explains their reduced A_{can}.

The ability of light-green canopies to increase *A* when L_R is reduced to a negligible value may help explain why Chl reductions in algal cultures have resulted in increased photosynthesis and growth culture (Melis, 1999; Polle et al., 2003; Mitra and Melis, 2008; Kirst et al., 2012). In *Chlorella* cultures, light absorption is well represented by the Beer-Lambert law at a variety of cellular densities, without the necessity for consideration of reflectance (Lee, 1999). The difference in reflective properties between a leaf and an algal culture could be the result of both the decreased differences in refractive indices between the algal cell (1.047-1.092, Spinrad and Brown, 1986) and the aqueous culture medium (1.33) compared to leaves and the less cell-dense culture conditions, which minimize cell-to-medium light scattering. For example, in the experiments of Kirst et al. (2012), reported improved growth of *Chlamydomonas reinhardtii* with reduced antenna complexes, cells were cultured at densities 1-3 $x10^6$ cells mL^{-1}. Leaf cell density is not reported directly, but can be approximated based on available data. Based on anatomical data, a single soybean leaf has ~2.5 $x10^6$ cells cm^{-2} in the palisade layers alone (Dornhoff and Shibles, 1976). Spongy mesophyll cells are smaller than palisade cells but are not packed as tightly. Assuming their cellular density per leaf surface area is similar to palisade cells, this means that a single leaf layer has a similar order of magnitude of light-scattering cells as a cm^3

of algal culture. Additionally, leaves are arranged in a variety of angles relative to each other, which would further serve to increase canopy light scattering. Due to these fundamental differences between the culture properties of algae and plants, it is impossible to completely separate L_R from L_T, but even reducing the relationship between the two would increase A_{can} in reduced-Chl canopies relative to canopies with L_R according to Equation 2.

Theoretically, L_T and L_R could be separated from each other if internal leaf architecture were simplified to limit the amount of cell-to-air interfaces. This could be accomplished by decreasing the cell number or complexity of the intercellular airspace, such as is seen in the *reticulata* mutants in Arabidopsis (González-Bayán et al., 2006). However this may negatively impact the efficiency of internal CO_2 diffusion and subsequent leaf photosynthesis (Syvertsen et al., 1995; Evans and von Caemmerer, 1996; Flexas et al., 2007).

The relationship between Chl and photosynthetic capacity gives insight to past work with light green canopies

We identified an important correlation between Chl and photosynthetic biochemical capacity (J_{max} and V_{cmax}) found in naturally- and chemically-derived soybean accessions that drastically alters the impact of Chl reduction on canopy performance (Figure 3 and 8, Supplemental 8, 9 and 11). The correlation between Chl and V_{cmax} had a higher y-intercept and lower slope than a relationship based on predicted nitrogen content and secondary relationships, suggesting that the Houborg *et al.* 2013 model may not apply well at least to soybean. The driver linking Chl to J_{max} and V_{cmax} is currently not known, but there were cultivars that had reduced Chl without a corresponding decrease in photosynthetic biochemical capacity in the 45 lines we surveyed with gas exchange (Figure 3). A similar inconsistent relationship between Chl and biochemical capacity was seen across soybean cultivars with years of release dates between 1923 and 2007 (Koester et al., 2016). The presence of accessions with high biochemical capacity and low Chl indicates there is not an underlying genetic linkage or immutable mechanism that links the two, and that the correlation can be avoided. The relationship between Chl and photosynthetic biochemical capacity found in naturally- and chemically-derived soybean accessions would

570 hamper efforts to breed for reduced chlorophyll production lines through traditional methods
571 and highlights the need for targeted genetic markers or genetic engineering.
572 While our findings show that, in general, Chl is correlated with biochemical performance
573 measured as V_{cmax} and J_{max} across a broad panel of soybean mutant accessions, the case may be
574 different in other species and dependent on the genetic and biochemical source of the
575 mutation. A rice mutant with greatly reduced Chl was reported to have large *increases* in both
576 V_{cmax} and J_{max} (Gu et al., 2017a; Gu et al., 2017b). Canopies of this mutant had significant
577 increases in A_{can}. The differences between our results in soybean and this single mutant in rice
578 could indicate species-specific differences in how nitrogen is re-partitioned when chlorophyll
579 production is impaired, or simply that the mutant they used for their study represents an
580 exception to the general trend. Our simulations predict that the increased A_{can} of this light
581 green rice cultivar was likely due more to the increases in V_{cmax} and J_{max} and not from PPFD
582 redistribution. Indeed, the rice mutant has higher A_{leaf} at saturating irradiances, indicating that
583 the leaf capacity for photosynthesis was greater than WT.
584 Furthermore, a *Nicotiana tabacum* mutant with substantially reduced Chl also reported
585 an increase in biomass yield when grown in dense stands (Kirst et al., 2017). The discrepancy
586 between this modeling work in soybean and this recent report in *N. tabacum* could be
587 attributed to a variety of reasons. Our simulations were parameterized specifically for field-
588 grown soybean, and differences in leaf thickness, arrangement and weather conditions (the *N.*
589 *tabacum* was grown in a greenhouse) could impact the results. Additionally, the *N. tabacum*
590 mutants were harvested several days after the wild type to make up for developmental
591 differences, which could confound the interpretation of the measured increases in biomass.
592 Taken at face value, our simulations indicate that the increase in growth found in *N. tabacum*
593 likely resulted from factors other than just canopy PPFD redistribution, such as developmental
594 differences or increases in V_{cmax} and/or J_{max} as was found in the rice cultivar.
595
596 *Pleiotropic effects of Chl reduction*
597 Since past work with *Y11y11* indicates that chlorophyll reduction can be accompanied with an
598 increase in stomatal conductance (Campbell et al., 2015; Slattery et al., 2017), what other

599 pleiotropic effects might be expected from reduced chlorophyll mutants? Chlorophyll
600 precursors are derived from the isoprenoid pathway, which also is involved in the biosynthesis
601 of a myriad of plant secondary metabolites including carotenoids, giberellins and tocopherols
602 (Lange and Ghassemian, 2003). Since chlorophyll reduction could be caused by any
603 perturbation downstream of final chlorophyll biosynthesis, it is possible that molecules that
604 share chlorophyll's biosynthetic pathway could be impacted in reduced chlorophyll plants. For
605 example, there was a strong correlation between Chl and total carotenoid content
606 (Supplemental 2a) that resulted in more carotenoids per chlorophyll at low Chl (Supplemental 2
607 similar to the relationship found in *Coffea canephora* Pierre leaves (Netto et al., 2005).
608 Carotenoids play a role in regulating non-photochemical quenching and harvesting light energy
609 in spectral regions that chlorophyll does not absorb strongly (Ort, 2001; Telfer et al., 2008),
610 indicating that these processes might be impacted in low Chl mutants. Interestingly, lower
611 carotenoid content also correlates with ABA levels in plants with transgenically-impaired
612 carotenoid synthesis (Lindgren et al., 2003). While ABA triggers stomatal closure (Farquhar and
613 Sharkey, 1982), the relationship between carotenoid content and stomatal closure was not
614 apparent in the 45 accessions that were examined via gas exchange (Supplemental 5a). Chl
615 reduction may also reduce the quantity of reactive oxygen species generated from over-excited
616 reaction centers (Vass and Cser, 2009) by reducing total light energy absorption, perhaps
617 resulting in surplus antioxidant capacity and improved stress response (Foyer and Shigeoka,
618 2011).

619 Conclusions

620 Our findings indicate that while reductions in Chl alone are not expected to increase *A* in
621 soybean, they can result in increased Φ_{CO2} and carbon fixation in individual domains of the
622 canopy. The inability of Chl reduction to increase canopy photosynthesis results primarily from
623 the fundamental linkage between L_R and L_T, with the vertical distribution of nitrogen being a
624 secondary factor. Nevertheless, our simulations show that canopies can assimilate similar
625 amounts of carbon dioxide with significant reductions in Chl. Future efforts should focus on re-

partitioning nitrogen from excess chlorophyll into more beneficial investments, such as V_{cmax} and J_{max}.

Materials and Methods

Field measurements for MLCan parameterization

Soybean germplasm (67 lines) with previously described "light green" phenotypes were planted in 1.5 meter rows using standard agronomic practice (Specific lines listed in Supplemental File 1). Seed was obtained from the United States Department of Agriculture Soybean germplasm collection (Urbana, IL) and from the Fast Neutron Soybean Mutagenesis Project (http://parrottlab.uga.edu/parrottlab/Mutagenesis/index.php) and when available, included the parental lines of the light green cultivar. Due to seed limitations, a single row of each variety was planted in a single randomized block, with edges bordered by WT (*Glycine max* Merr., cultivar “Clark”) rows. Leaves for analysis were harvested at two points in the growing season by pre-dawn cutting from the plant followed by re-cutting the petioles under water. Plants were then transferred in a darkened container to the lab for Chl, total carotenoid and optical property determination. L_R, L_T, L_A and SPAD (Chlorophyll Meter SPAD-502 Plus, Konica Minolta) were determined on 3-5 replicates of each line and Chl was determined on the same area using ethanol extraction (Ritchie, 2006). The relationship used to convert SPAD readings to Chl was calculated using an exponential function (Supplemental 13). Leaf optical properties were determined using an integrating sphere and spectroradiometer using a tungsten-halide source (Jaz Spectroclip, Ocean Optics, Dunedin, FL, USA) with a source in the visible range although it should be noted that the source has reduced output between ~400-500 nm, meaning that the measurements of blue light are less reliable than that for the other colors. The integrating sphere/spectroradiometer was first calibrated with a “Spactralon” 99% reflectance standard (Labsphere Inc, North Sutton, NH, USA) and the black standard included with the instrument. Dark-adapted and steady-state fluorescence were measured using a fluorescence camera on leaf disks placed on agar plates.

The relationships between leaf optics and Chl that were used to define leaf optical properties in MLCan as a function of Chl were:

$$Leaf_T = 0.228e^{-0.00288(Chl)} \quad \text{Equation 1}$$

($R^2 = 0.50$) and

$$Leaf_R = 0.208e^{-0.00217(Chl)} \quad \text{Equation 2}$$

($R^2 = 0.52$). The R^2 values of the relationships between Chl and leaf optics (Equations 1 and 2) indicate that there are factors impacting leaf optics other than Chl. This is to be expected given the diverse genetic nature of the soybean accessions measured and the complex interaction of leaf anatomy with incident PPFD (Osborne and Raven, 1986) as well as measurement noise. Indeed, past work measuring the relationship of Chl with L_A observe a similar degree of variance (Osborne and Raven, 1986; Evans and Poorter, 2001). For our simulations we assumed that these other factors would be constant in a leaf where only the Chl was reduced and used the above equations to simulate the impact of Chl on leaf optics.

The response of A_{leaf} to carbon dioxide concentration (A-C_i) was measured in the light green and parental cultivars to determine the relationship between Chl and photosynthetic biochemical capacity (V_{cmax} and J_{max}). A subset of 45 cultivars were selected with a wide variation in Chl for measurements and harvested by pre-dawn petiolar cutting and kept under partial (between 20-200 PPFD) illumination before measurements. A full A-C_i curve was measured for each cultivar using a LI-COR 6400XT (LI-COR Biosciences, Lincoln, NE, USA) and SPAD measured as a proxy for Chl. SPAD estimates of Chl based on the above calibration (Supplemental 13) were used since leaf samples were not harvested for direct determination. Measurements were made using a 2 cm^2 measuring area, a flow rate of 300 $\mu mol\ s^{-1}$, and CO_2 reference concentration sequence of 400, 300, 200, 100, 50, 400, 600, 800, 1000, 1300 and 400 PPM CO_2. The instrument's block temperature was maintained at 3° below ambient temperature resulting in leaf temperatures between 25-30° depending on the time of day the measurement was made. Measurements were randomized and limited to the hours between 9:00 and 14:00 to avoid end of day photosynthetic depression. V_{cmax} and J_{max} were determined by fitting A-C_i curves and normalized to 25°C using the temperature response of each determined previously for *N. tabacum* (Bernacchi et al., 2001; Bernacchi et al., 2002; Bernacchi

683 et al., 2003; Sharkey et al., 2007). The relationship between V_{cmax} and Chl produced from this
684 dataset was

685 $$V_{cmax} = 0.17(Chl) + 67.2$$ Equation 3

686

687 with an R^2 of 0.27, and the relationship between J_{max} and Chl was

688 $$J_{max} = 0.33(Chl) + 113.4$$ Equation 4

689

690 with an R^2 of 0.54.

691 Leaf nitrogen content was measured in field-harvested samples of WT and *Y11y11* from
692 the 2013 season on 5 different growing days. Samples were oven dried for three days and
693 ground using a ball mill (Geno Grinder 2010, BT&C Lebanon, New Jersey, USA) and analyzed
694 using an elemental analyzer (Costech 4010CHNSO Analyzer, Costech Analytical Technologies
695 Inc. Valencia, California, USA). Acetanalide (National Institute of Science and Technology,
696 Gaithersburg, Maryland, USA) were used as standards.

697 Leaf soluble protein content was determined by Bradford method (Bradford, 1976).
698 Samples (1-cm diameter leaf disk) were collected in three plots during the 2013 season over
699 four growing days. Tissues were rapidly frozen in liquid nitrogen, stored at -80°C and ground by
700 using glass homogenizer while frozen. After extraction buffer was added, extracts were
701 centrifuged at 18,000 x g at 4°C for 5 min. Supernatants were collected and mixed with Bio-Rad
702 protein assay dye (Bio-Rad, Hercules, California, USA). Absorbance of samples along with bovine
703 serum albumin as standard was measured at 595 nm by microplate reader (BioTek, Winooski,
704 Vermont, USA).

705

706 *Implementing the impact of Chl into MLCan*

707 MLCan treats PAR as a single broadband radiation stream by dividing total downwelling
708 radiation between long and shortwave, then further partitioning shortwave radiation between
709 PAR and near infra-red (Campbell and Norman, 1998; Drewry et al., 2010a). We measured leaf
710 optical properties (L_R, L_T and L_A) at ~0.34 nm resolution across the PAR portion of the spectrum
711 (400-700 nm), requiring us to aggregate leaf spectral properties to broadband PPFD values. To

712 do this, L_R, L_T and L_A were averaged into 25 nm increments between 400-700 nm. 25 nm was
713 selected as an interval since it gave reasonable resolution across both the chlorophyll
714 absorption spectra and the solar spectra for weighted averaging. L_R, L_T and L_A for each 25 nm
715 value were then multiplied by the percentage of solar radiation incident relative to the total
716 PAR solar radiation using a reference solar spectrum, to produce weighted values (L_R, L_T and L_A,
717 ASTM, 2012). The weighted L_R, L_T and L_A values from each 25 nm increment were then summed
718 to produce a weighted average across the PAR spectrum, which was then fit to produce
719 empirical allometric relationships between optical properties and Chl (Equations 1 and 2).
720 Equations 1 and 2 were used to vary leaf-level optics based on the value of Chl used in
721 MLCan. To accomplish this, MLCan was modified so that L_R, L_T and L_A were varied for each 30
722 min time step, instead of being assigned as constant default values. In the first series of
723 simulations representing WT and *Y11y11* canopies, time step-specific Chl where interpolated
724 from values measured for each genotype throughout the growing season (Slattery et al., 2017).
725 L_R and L_T were calculated for each time step using equations 1 and 2, and L_A determined
726 according to 1 - L_R – L_T.
727 Since the relationships of L_R and L_T were determined as a function of Chl, MLCan was
728 modified to incorporate the individual relationships of both. MLCan, like many canopy models,
729 assumes that L_R is equal to L_T, which simplifies the derivation of the extinction and scattering of
730 radiation throughout the canopy. Leaf-level optics were scaled to the canopy-layer level by
731 using a PPFD extinction (K_h) and reflectance (ρ_h) coefficient that considered L_R was not equal to
732 L_T, allowing us to individually vary both parameters. Specifically, the original MLCan formulation
733 of

734 $$K_h = (1-\sigma)^{0.5} \qquad \text{Equation 5,}$$

735 where σ represents a scattering coefficient equal to L_R + L_T and assuming L_R = L_T, was replaced
736 with

737 $$K_h = \left([1-\mathrm{Leaf_T}]^2 - \mathrm{Leaf_R}^2\right)^{0.5} \qquad \text{Equation 6}$$

738 and

739 $$\rho_h = \frac{1-(1-\sigma)^{0.5}}{1+(1-\sigma)^{0.5}} \qquad \text{Equation 7}$$

740 was replaced with

741 $$\rho_h = \frac{(1-\mathrm{Leaf_T}-K_h)^{0.5}}{\mathrm{Leaf_R}}$$ Equation 8.

742 Details on the derivation of the equations and their use in MLCan can be found in (Goudriaan,
743 1977, Equations 2.20-23) and Drewry et al. (2010a, Supplemental Equation 23). For each time-
744 step, radiation was distributed through the canopy iteratively until all incoming radiation was
745 either absorbed by a canopy layer or the soil, or reflected into the atmosphere to account for
746 the inter-canopy scattering and absorbance of incoming light. Soil reflectance was assumed to
747 be 0.2.

748 In simulations including a scaling of V_{cmax} and J_{max} with Chl, leaf biochemistry was
749 modified as a function of Chl for each time step using the empirical measurements according to
750 equations 3 and 4. This did not impact the simulations where Chl was constant throughout the
751 growing season, but did have an impact when the WT and *Y11y11* canopies were simulated
752 using field-measured seasonal Chl values. In all simulations Chl was considered constant
753 through the canopy with no developmental-dependent effects. The vertical distribution of Chl
754 was not accounted meaning that all leaves had the same assumed Chl for a given time step. For
755 simulations determining the impact of uncoupling L_R from L_T, L_R in equation 2 was maintained at
756 a constant value for Chl of 450 μmol m^{-2}, while L_T varied according to equation 1 and L_A
757 determined as 1 - L_R – L_T. All meteorological, physiological and ecological data are available by
758 contacting author BJW. For access to MLCan code, contact DTD.
759
760 *Simulations comparing a WT and* Y11y11 *canopy*
761 Field measurements from the 2013 growing season were used to parameterize the canopy
762 simulations of WT and *Y11y11* soybean canopies. Seasonal leaf area density, LAI, and Chl were
763 taken from field measurements as reported previously (Slattery et al., 2017). Photosynthetic
764 biochemical parameters (V_{cmax} and J_{max}) were assumed as outlined in the various modeled
765 scenarios. Precipitation data were taken from the nearby Willard Airport weather station and
766 radiation, windspeed, and temperature from other nearby sources as reported previously
767 (Bagley et al., 2015).

768 It was a particularly wet spring with little additional precipitation during the growing
769 season and the modeled soil moisture drove an end-of-season modeled stomatal closure.

Modeled soil moisture did not agree well with field measurements, so the soil-model was constrained to never drop below measured values in the *Y11y11* or the full Chl simulations. Soil moisture was measured on a biweekly basis in a nearby plot of soybean (*cv.* Pana, PI 597387) using a capacitance probe (Diviner-2000, Sentek Sensor Technologies) inserted into access tubes. Measurements were made in three access tubes at 10 cm increments between depths of 5 and 105 cm and averaged together to constrain the model. The raw data were converted to gravimetric data using a calibration determined in prepared soils (Paltineanu and Starr, 1997).

Simulating the impact of a range of Chl and nitrogen distribution on canopy performance

To determine canopy performance under a wider range of Chl the 2013 season was simulated using Chl ranging from 25 to 500 μmol m^{-2}. This simulation was done both assuming and not assuming that V_{cmax} and J_{max} scale according to Chl and assuming that L_R was maintained at a value calculated when Chl = 450 μmol m^{-2} (Equation 2).

The impact of changes to the distribution profile of nitrogen to canopy performance was investigated in MLCan by altering the coefficient for the exponential function that represents the distribution of nitrogen through the canopy. Specifically, MLCan represents the canopy nitrogen profile, which scales V_{cmax} and J_{max} through the canopy as a function of nitrogen, according to the relationship

$$V_{cmax}(\xi) = {V_{cmax}}^{top} \exp[-k_n * \xi] \qquad \text{Equation 9}$$

where ξ, V_{cmax} and ${V_{cmax}}^{top}$ is equal to the cumulative LAI, V_{cmax} at the layer being modeled and the V_{cmax} at the top of the canopy respectively (De Pury and Farquhar, 1997). In order not to include the effects of having more or less total nitrogen in a canopy as a result of changing k_n, MLCan was amended to use the relationship above with the default value of k_n = 0.5 to first produce a baseline canopy nitrogen content. This baseline total nitrogen content was then scaled according to the relationship above to produce canopies with the same total amount of nitrogen but different profiles.

Acknowledgments

Jessica Ayers, Beau Barber, Kaitlin Togliatti and Elliot Brazil for assistance sampling and measuring the population of reduced Chl cultivars. Christopher Montes for providing the soil moisture data from an adjoining plot at the Soybean Free Air Concentration Enrichment site. Randall Nelson (Retired) of the USDA for providing the light green Soybean accessions. Anastasiia Bovdilova for providing Russian translation of early references to light green in the literature.

Figure Legends

Figure 1: Examples of some of the 67 soybean lines with decreased chlorophyll content (a). Leaf punches prepared for chlorophyll fluorescence imaging (b). Most of the lines were obtained from the USDA soybean germplasm collection and others from the Fast Neutron Soybean Mutagenesis project. Lines were characterized for chlorophyll content, leaf transmittance and leaf reflectance.

Figure 2: Shown are the relationships between leaf chlorophyll content and reflectance (L_R, a), transmittance (L_T, b) and absorbance (L_A, c) across the spectrum of photosynthetically active radiation.

Figure 3: Observed impact of the variation in chlorophyll content (Chl) on photosynthetic performance. 45 plants from various cultivars of soybean were measured using a LI-COR 6400-XT gas exchange system to derive maximum rate of carboxylation (V_{cmax}) and electron transport (J_{max}) from photosynthetic carbon dioxide response curves. Chl was determined from SPAD measurements according to the relationship presented in Supplemental 12. Also shown is the modeled relationship of Chl to V_{cmax} of Houborg 2013 (dotted line). Circled data represents the values measured in the low chlorophyll mutant *Y11y11*.

Figure 4: Vertically-resolved, diurnal differences in absorbed PPFD ($\Delta PPFD_A$; a and b), net photosynthetic CO_2 assimilation (ΔA; c and d), and the quantum efficiency of CO_2 assimilation ($\Delta\Phi_{CO2}$; e and f) between a mutant with reduced chlorophyll content (*Y11y11*) and wild-type (WT) before canopy closure early in the growing season (DOY 193 LAI =2.7: a, c and e) and at peak LAI (DOY 230 LAI=7.5: b, d and f). Color maps shows the difference between *Y11y11* and WT canopies (*Y11y11* - WT values) at each of the vertical canopy regions above ground normalized by the canopy height (z/h). Positive values (yellow / red) represent regions of the canopy where *Y11y11* has a larger value than WT, and blue values are regions where the WT values are higher. The two selected days were both cloudless and received similar amounts of total downwelling radiation (Supplemental 5). Wild-type and *Y11y11* canopies were parameterized using genotype-specific chlorophyll contents and leaf area indices. Values are expressed on a ground area basis.

Figure 5: Vertically resolved differences in absorbed photosynthetically active radiation ($\Delta PPFD_A$, a) and net CO_2 assimilation (Δ A, c) between a simulated soybean canopy with reduced chlorophyll content (*Y11y11*) and a wild-type (WT) canopy, at mid-day time points for days of year (DOY) spanning the growing season. Vertical profiles (height above ground normalized by canopy height, z/h) are presented for midday periods (1:00PM) of each day throughout the growing season. Also shown are the seasonally-integrated values for $PPFD_A$ (b) and *A* (d). Color map shows the difference between *Y11y11* and WT canopies (*Y11y11* - WT values) at each of the canopy regions, normalized by the canopy height (z/h). Positive values (more red) represent regions of the canopy where *Y11y11* has a larger value than WT, and more blue values are regions where the WT values are higher. These simulations were driven by field-measured incident radiation, temperatures, and precipitation (see Supplementary Figure 5). Wild-type and *Y11y11* canopies were parameterized using genotype-specific chlorophyll contents and leaf area indices (Slattery 2017).

Figure 6: Season long differences in the midday quantum efficiency of CO_2 assimilation ($\Delta\Phi_{CO2}$) between *Y11y11* soybean mutants (*Y11y11*) and wild-type (WT) across the vertical profile of the

852 canopies (height above ground normalized by canopy height, z/h) for the 2013 growing season.
853 Color map shows the difference between *Y11y11* and WT canopies (*Y11y11* - WT) at each of the
854 canopy regions above ground normalized by the canopy height (z/h). Positive values (more red)
855 represent regions of the canopy where *Y11y11* has a larger value than WT, and more blue
856 values are regions where the WT values are higher. Simulations were performed assuming the
857 genotype-specific chlorophyll content (Chl) and *Y11y11* values for leaf area index (LAI) and
858 constant photosynthetic biochemical capacity (V_{cmax} and J_{max}; a), WT LAI and biochemical
859 capacity scaled with Chl (b), WT LAI and a constant photosynthetic biochemical capacity (c) and
860 *Y11y11* values for LAI and biochemical capacity scaled with Chl (d). Environmental forcing
861 (precipitation, downwelling radiation, temperature, H_2O vapor pressure and wind speed) for
862 the simulations were taken from the 2013 growing-season.
863
864 Figure 7**:** Total canopy reflectance (Can_R; a and b), transmittance (Can_T; c and d) and absorbance
865 (Can_A; e and f) in simulated canopies composed of a range of leaf chlorophyll contents (Chl)
866 going from dark green (500 μmol m^{-2}) to light green (50 μmol m^{-2}) according to DOY within the
867 growing season. Total values for each optical property were determined by summing the
868 diurnal values for PPFD reflected, transmitted or absorbed by the canopy divided by the
869 summed total of diurnal incoming PPFD. Simulations were performed assuming leaf reflectance
870 ($Leaf_R$)and transmittance ($Leaf_T$) co-varied according to empirical relationships (a, c, e; Equation
871 1 and 2) derived from observations of diverse soybean lines (see Figure 2) spanning a wide
872 range of Chl as indicated by the decreasing Chl displayed on the y-axis. Alternatively, canopies
873 were simulated with $Leaf_R$ set to a negligible value at every Chl (b, d and f) to show the impact
874 of leaf reflective loss on total canopy optical properties.
875
876 Figure 8 Impact of chlorophyll content (Chl) reduction on the seasonal simulated soybean
877 photosynthesis (A_{can}; a) and the quantum efficiency of CO_2 fixation (Φ_{CO2}; b). Seasonal values
878 are shown for the 2013 growing season (see Supplemental Figure 5). Simulations were
879 performed assuming leaf photosynthetic biochemical capacity remained constant despite
880 chlorophyll content (Chl; circles) or that it scaled with Chl according to Equations 3 and 4

(squares). Leaf reflectance and transmittance were also assumed to both vary with Chl according to Equations 1 and 2 (filled symbols) or leaf reflectance remained constant despite changes in Chl (open symbols) to determine the impact of changes in reflective loss on canopy performance.

Figure 9: The response of total daily canopy carbon assimilation (A_{can}) to different assumptions of chlorophyll content (Chl) and canopy nitrogen distribution profiles. Canopy nitrogen profiles were adjusted through varying k_n, a term describing the exponential decay of nitrogen through a canopy profile (See Supplemental 7 and Materials and Methods for more detail). Environmental forcing (radiation, temperature, relative humidity...etc) was taken as the average daily conditions for the 2013 growing season. Shown are the relationships between Chl, nitrogen distribution and canopy A assuming leaf reflectance ($Leaf_R$)and transmittance ($Leaf_T$) co-varied according to empirical relationships (a) and assuming $Leaf_R$ was negligible (b).

Supplemental Data

Supplemental Figure 1: Ratio of leaf transmittance (L_T) to reflectance (L_R) as a function of chlorophyll content

Supplemental Figure 2: Relationship between chlorophyll content (Chl) and total carotenoid content (a) and the ratio of carotenoid to Chl across the 67 reduced-Chl accessions as measured on two separate field days

Supplemental Figure 3: Relationship between chlorophyll content (Chl) and leaf reflectance ($Leaf_R$, a) and transmittance ($Leaf_T$, b) determined from 67 soybean accessions with varying amounts of Chl.

Supplemental Figure 4: Relationship between maximum variable fluorescence and electron transport rate

Supplemental Figure 5: Impact of variation in chlorophyll content (Chl) on stomatal conductance (g_s) and rates of day respiration (R_d) in 45 plants from various cultivars of soybean as measured by fitting photosynthetic CO_2 response curves

Supplemental Figure 6**:** Season-long incident Photosynthetic Photon Flux Density (PPFD; a), air temperature (b), precipitation (c) and H_2O vapor pressure (d) as measured in (Slattery *et al* 2017) and used to parameterize our season-long simulations

Supplemental Figure 7: Seasonal values for measured leaf nitrogen (N), measured chlorophyll content (Chl), calculated nitrogen associated with Chl (N in Chl; g m^{-2}), and a lower bounds calculation of the percent leaf nitrogen associated with Chl (N in Chl; %) for each day of year (DOY).

Supplemental Figure 8: Diurnal differences in absorbed PPFD ($\Delta PPFD_A$; a and b), net photosynthetic CO_2 assimilation (ΔA; c and d), and the quantum efficiency of CO_2 assimilation ($\Delta\Phi_{CO2}$; e and f) between canopies with chlorophyll content (Chl)=400 and Chl = 200 representing Wild-type and reduced Chl mutants.

Supplemental Figure 9: Diurnal differences in absorbed PPFD radiation ($\Delta PPFD_A$; a and b), net photosynthetic CO_2 assimilation (ΔA; c and d), and the quantum efficiency of CO_2 assimilation ($\Delta\Phi_{CO2}$; e and f) between canopies with chlorophyll content (Chl)=400 and Chl = 200 representing Wild-type and reduced Chl mutants.

Supplemental Figure 10: Season long relationships between the daily midday differences in the quantum efficiency of CO_2 assimilation ($\Delta\Phi_{CO2}$) between *Y11y11* soybean mutants and wild-type (WT) and net carbon assimilation (A_n; a) and absorbed photosynthetic photon flux density ($PPFD_A$; b)

Supplemental Figure 11**:** Impact of chlorophyll content (Chl) reduction on carbon fixation in simulated soybean canopies

Supplemental Figure 12: Impact of changes to the coefficient of nitrogen distribution (k_n) on the vertical distribution of nitrogen through the canopy profile compared to the Photosynthetic Photon Flux Density (PPFD) absorbed normalized to the uppermost canopy layer of nitrogen partitioning or absorption

Supplemental Figure 13: Relationship between SPAD and chlorophyll content (Chl) as measured in various soybean cultivars with differing Chl

Supplemental Data: Cultivars and Gas Exchange Measurements

941
942
943
944 Supplemental 1: Ratio of leaf transmittance (L_T) to reflectance (L_R) as a function of chlorophyll
945 content (Chl) across mutants with reduced leaf Chl shown as a function of Chl (a) and as an
946 average of all Chl with standard deviations indicated by the grayed area and a 1:1 ratio
947 indicated by the blue line (b).
948
949 Supplemental 2: Relationship between chlorophyll content (Chl) and total carotenoid content
950 (a) and the ratio of carotenoid to Chl across the 67 reduced-Chl accessions as measured on two
951 separate field days.
952
953 Supplemental 3: Relationship between chlorophyll content (Chl) and leaf reflectance ($Leaf_R$, a)
954 and transmittance ($Leaf_T$, b) determined from 67 soybean accessions with varying amounts of
955 Chl.
956
957 Supplemental 4: Relationship between maximum variable fluorescence (F_v/F_m; a) and electron
958 transport rate (ETR; b) estimated by imaging dark-adapted leaf punches of soybean mutants
959 with decreased chlorophyll content (Chl) using a chlorophyll fluorescence imager.
960
961 Supplemental 5: Impact of variation in chlorophyll content (Chl) on stomatal conductance (g_s)
962 and rates of day respiration (R_d) in 45 plants from various cultivars of soybean as measured by
963 fitting photosynthetic CO_2 response curves.
964
965 Supplemental 6**:** Season-long incident Photosynthetic Photon Flux Density (PPFD; a), air
966 temperature (b), precipitation (c) and H_2O vapor pressure (d) as measured in (Slattery *et al*
967 2017) and used to parameterize our season-long simulations. Also shown are the Leaf Area
968 Indices (LAI, e) and chlorophyll contents (Chl; f) used to simulate the wild-type (WT) or *Y11y11*
969 canopies in figures 4 and 5.

970

971 Supplemental 7: Seasonal values for measured leaf nitrogen (N), measured chlorophyll content
972 (Chl), calculated nitrogen associated with Chl (N in Chl; g m^{-2}), and a lower bounds calculation of
973 the percent leaf nitrogen associated with Chl (N in Chl; %) for each day of year (DOY).
974

975 Supplemental 8: Diurnal differences in absorbed PPFD ($\Delta PPFD_A$; a and b), net photosynthetic
976 CO_2 assimilation (ΔA; c and d), and the quantum efficiency of CO_2 assimilation ($\Delta\Phi_{CO2}$; e and f)
977 between canopies with chlorophyll content (Chl)=400 and Chl = 200 representing Wild-type and
978 reduced Chl mutants.
979

980 Supplemental 9: Diurnal differences in absorbed PPFD radiation ($\Delta PPFD_A$; a and b), net
981 photosynthetic CO_2 assimilation (ΔA; c and d), and the quantum efficiency of CO_2 assimilation
982 ($\Delta\Phi_{CO2}$; e and f) between canopies with chlorophyll content (Chl)=400 and Chl = 200
983 representing Wild-type and reduced Chl mutants.
984

985 Supplemental 10: Season long relationships between the daily midday differences in the
986 quantum efficiency of CO_2 assimilation ($\Delta\Phi_{CO2}$) between *Y11y11* soybean mutants and wild-
987 type (WT) and net carbon assimilation (A_n; a) and absorbed photosynthetic photon flux density
988 ($PPFD_A$; b).
989

990 Supplemental 11**:** Impact of chlorophyll content (Chl) reduction on carbon fixation in simulated
991 soybean canopies.
992

993 Supplemental 12: Impact of changes to the coefficient of nitrogen distribution (k_n) on the
994 vertical distribution of nitrogen through the canopy profile compared to the Photosynthetic
995 Photon Flux Density (PPFD) absorbed normalized to the uppermost canopy layer of nitrogen
996 partitioning or absorption (See Materials and Methods for details on k_n).
997

Supplemental 13: Relationship between SPAD and chlorophyll content (Chl) as measured in various soybean cultivars with differing Chl.

Citations

Ainsworth EA, Rogers A, Leakey ADB, Heady LE, Gibon Y, Stitt M, Schurr U (2007) Does elevated atmospheric [CO_2] alter diurnal C uptake and the balance of C and N metabolites in growing and fully expanded soybean leaves? Journal of Experimental Botany **58:** 579-591

Anten NPR (1997) Modelling canopy photosynthesis using parameters determined from simple non-destructive measurements. Ecological Research **12:** 77

Anten NPR, Schieving F, Werger MJA (1995) Patterns of light and nitrogen distribution in relation to whole canopy carbon gain in C3 and C4 mono- and dicotyledonous species. Oecologia **101:** 504-513

Archontoulis SV, Vos J, Yin X, Bastiaans L, Danalatos NG, Struik PC (2011) Temporal dynamics of light and nitrogen vertical distributions in canopies of sunflower, kenaf and cynara. Field Crops Research **122:** 186-198

ASTM (2012) Standard Tables for Reference Solar Spectral Irradiances: Direct Normal and Hemispherical on 37° Tilted Surface. *In*, West Conshohocken, PA

Bagley J, Rosenthal DM, Ruiz-Vera UM, Siebers MH, Kumar P, Ort DR, Bernacchi C (2015) The influence of photosynthetic acclimation to rising CO_2 and warmer temperatures on leaf and canopy photosynthesis models. Global Biogeochemical Cycles **29:** 194-206

Baker NR (2008) Chlorophyll fluorescence: a probe of photosynthesis *in vivo*. Annual Review of Plant Biology **59:** 89-113

Baldocchi DD, Wilson KB, Gu L (2002) How the environment, canopy structure and canopy physiological functioning influence carbon, water and energy fluxes of a temperate broad-leaved deciduous forest- an assessment with the biophysical model CANOAK. Tree Physiology **22:** 1065-1077

Bernacchi CJ, Pimentel C, Long SP (2003) *In vivo* temperature response functions of parameters required to model RuBP-limited photosynthesis. Plant, Cell & Environment **26:** 1419-1430

Bernacchi CJ, Portis AR, Nakano H, von Caemmerer S, Long SP (2002) Temperature response of mesophyll conductance. Implications for the determination of Rubisco enzyme kinetics and for limitations to photosynthesis *in vivo*. Plant Physiology **130:** 1992-1998

Bernacchi CJ, Singsaas EL, Pimentel C, Portis AR, Long SP (2001) Improved temperature response functions for models of Rubisco-limited photosynthesis. Plant Cell & Environment **24:** 253-259

Campbell BW, Mani D, Curtin SJ, Slattery RA, Michno J-M, Ort DR, Schaus PJ, Palmer RG, Orf JH, Stupar RM (2015) Identical substitutions in magnesium chelatase paralogs result in chlorophyll-deficient soybean mutants. G3: Genes|Genomes|Genetics **5:** 123-131

Campbell G, Norman J (1998) Introduction to environmental biophysics. Springer Verlag

De Pury D, Farquhar GD (1997) Simple scaling of photosynthesis from leaves to canopies without the errors of big-leaf models. Plant Cell & Environment **20:** 537-557

Del Pozo A, Dennett MD (1999) Analysis of the distribution of light, leaf nitrogen, and photosynthesis within the canopy of Vicia faba L. at two contrasting plant densities. Australian Journal of Agricultural Research **50:** 183-190

Dornhoff GM, Shibles R (1976) Leaf morphology and anatomy in relation to CO_2-exchange rate of soybean leaves. Crop Science **16:** 377-381

Dreccer MF, van Oijen M, Schapendonk AHCM, Pot CS, Rabbinge R (2000) Dynamics of vertical leaf nitrogen distribution in a vegetative wheat canopy. Impact on canopy photosynthesis. Annals of Botany **86:** 821-831

Drewry DT, Kumar P, Long S, Bernacchi C, Liang XZ, Sivapalan M (2010a) Ecohydrological responses of dense canopies to environmental variability: 1. Interplay between vertical structure and photosynthetic pathway. Journal of Geophysical Research: Biogeosciences **115:** G04022

Drewry DT, Kumar P, Long S, Bernacchi C, Liang XZ, Sivapalan MCG (2010b) Ecohydrological responses of dense canopies to environmental variability: 2. Role of acclimation under elevated CO_2. Journal of Geophysical Research: Biogeosciences **115:** G04023

Drewry DT, Kumar P, Long SP (2014) Simultaneous improvement in productivity, water use, and albedo through crop structural modification. Global Change Biology **20:** 1955-1967

Evans JR, Poorter H (2001) Photosynthetic acclimation of plants to growth irradiance: the relative importance of specific leaf area and nitrogen partitioning in maximizing carbon gain. Plant, Cell & Environment **24:** 755-767

Evans JR, Seemann JR (1989) The allocation of protein nitrogen in the photosynthetic apparatus: costs, consequences, and control. Photosynthesis**:** 183-205

Evans JR, von Caemmerer S (1996) Carbon dioxide diffusion inside leaves. Plant Physiology **110:** 339-346

Farquhar GD, Sharkey TD (1982) Stomatal conductance and photosynthesis. Annual Review of Plant Physiology **33:** 317-345

Field C (1983) Allocating leaf nitrogen for the maximization of carbon gain: leaf age as a control on the allocation program. Oecologia **56:** 341-347

Flexas J, Ortuño MF, Ribas-Carbo M, Diaz-Espejo A, Flórez-Sarasa ID, Medrano H (2007) Mesophyll conductance to CO_2 in *Arabidopsis thaliana*. New Phytologist **175:** 501-511

Foyer CH, Shigeoka S (2011) Understanding oxidative stress and antioxidant functions to enhance photosynthesis. Plant Physiology **155:** 93-100

González-Bayán R, Kinsman EA, Quesada V, Vera A, Robles P, Ponce MR, Pyke KA, Micol JL (2006) Mutations in the RETICULATA gene dramatically alter internal architecture but have little effect on overall organ shape in Arabidopsis leaves. Journal of Experimental Botany **57:** 3019-3031

Goudriaan J (1977) Crop micrometeorology: a simulation study. Pudoc, Wageningen

Gu J, Zhou Z, Li Z, Chen Y, Wang Z, Zhang H (2017a) Rice (*Oryza sativa* L.) with reduced chlorophyll content exhibit higher photosynthetic rate and efficiency, improved canopy light distribution, and greater yields than normally pigmented plants. Field Crops Research **200:** 58-70

Gu J, Zhou Z, Li Z, Chen Y, Wang Z, Zhang H, Yang J (2017b) Photosynthetic properties and potentials for improvement of photosynthesis in pale green leaf rice under high light conditions. Frontiers in Plant Science **8**

Gutschick V (1984a) Photosynthesis model for C_3 leaves incorporating CO_2 transport, radiation propagation, and biochemistry. 1. Kinetics and their parametrization. Photosynthetica **18:** 549-568

Gutschick V (1984b) Photosynthesis model for C3 leaves incorporating CO2 transport, radiation propagation, and biochemistry. 2. Ecological and agricultural utility. Photosynthetica **18:** 569-595

Gutschick V (1988) Optimization of specific leaf mass, internal CO_2 concentration, and chlorophyll content in crop canopies. Plant Physiology and Biochemistry **26:** 525-537

Hikosaka K, Niinemets U, Anten NP (2016) Canopy photosynthesis: from basics to applications. Springer

Hikosaka K, Terashima I (1995) A model of the acclimation of photosynthesis in the leaves of C3 plants to sun and shade with respect to nitrogen use. Plant, Cell & Environment **18:** 605-618

Kirst H, Gabilly ST, Niyogi KK, Lemaux PG, Melis A (2017) Photosynthetic antenna engineering to improve crop yields. Planta**:** 1-12

Kirst H, Garcia-Cerdan JG, Zurbriggen A, Ruehle T, Melis A (2012) Truncated photosystem chlorophyll antenna size in the green microalga *Chlamydomonas reinhardtii* upon deletion of the TLA3-CpSRP43 gene. Plant Physiology **160:** 2251-2260

Koester RP, Skoneczka JA, Cary TR, Diers BW, Ainsworth EA (2016) Historical gains in soybean (*Glycine max* Merr.) seed yield are driven by linear increases in light interception, energy conversion, and partitioning efficiencies. Journal of Experimental Botany **65:** 3311-3321

Kromdijk J, Long SP (2016) One crop breeding cycle from starvation? How engineering crop photosynthesis for rising CO_2 and temperature could be one important route to alleviation. Proceedings of the Royal Society B: Biological Sciences **283**

Kuhlbrandt W, Wang DN, Fujiyoshi Y (1994) Atomic model of plant light-harvesting complex by electron crystallography. Nature **367:** 614-621

Lai C-T, Katul G, Oren R, Ellsworth D, Schäfer K (2000) Modeling CO_2 and water vapor turbulent flux distributions within a forest canopy. Journal of Geophysical Research: Atmospheres **105:** 26333-26351

Laisk A (1982) Correspondence of photosynthetic system to environmental conditions. *In* N AA, ed, Fiziologiya fotosinteza. Nauka, Moscow, pp 221-234

Lange BM, Ghassemian M (2003) Genome organization in Arabidopsis thaliana: a survey for genes involved in isoprenoid and chlorophyll metabolism. Plant Molecular Biology **51:** 925-948

Lee C-G (1999) Calculation of light penetration depth in photobioreactors. Biotechnology and Bioprocess Engineering **4:** 78-81

Leuning R, Kelliher FM, De Pury DGG, Schulze ED (1995) Leaf nitrogen, photosynthesis, conductance and transpiration: scaling from leaves to canopies. Plant Cell & Environment **18:** 1183-1200

Lindgren LO, Stålberg KG, Höglund A-S (2003) Seed-specific overexpression of an endogenous arabidopsis phytoene synthase gene results in delayed germination and increased levels of carotenoids, chlorophyll, and abscisic acid. Plant Physiology **132:** 779-785

Long SP, Marshall-Colon A, Zhu X-G (2015) Meeting the global food demand of the future by engineering crop photosynthesis and yield potential. Cell **161:** 56-66

Long SP, Zhu X-G, Naidu SL, Ort DR (2006) Can improvement in photosynthesis increase crop yields? Plant Cell & Environment **29:** 315-330

Melis A (1999) Photosystem-II damage and repair cycle in chloroplasts: what modulates the rate of photodamage in vivo? Trends in Plant Science **4:** 130-135

Mitra M, Melis A (2008) Optical properties of microalgae for enhanced biofuels production. Optics Express **16:** 21807-21820

Moreau D, Allard V, Gaju O, Le Gouis J, Foulkes MJ, Martre P (2012) Acclimation of leaf nitrogen to vertical light gradient at anthesis in wheat is a whole-plant process that scales with the size of the canopy. Plant Physiology **160:** 1479-1490

Netto AT, Campostrini E, Oliveira JGd, Bressan-Smith RE (2005) Photosynthetic pigments, nitrogen, chlorophyll a fluorescence and SPAD-502 readings in coffee leaves. Scientia Horticulturae **104:** 199-209

Niinemets Ü (2007) Photosynthesis and resource distribution through plant canopies. Plant, Cell & Environment **30:** 1052-1071

Niinemets Ü, Keenan TF, Hallik L (2015) A worldwide analysis of within-canopy variations in leaf structural, chemical and physiological traits across plant functional types. New Phytologist **205:** 973-993

Niinemets Ü, Tenhunen JD (1997) A model separating leaf structural and physiological effects on carbon gain along light gradients for the shade-tolerant species Acer saccharum. Plant, Cell & Environment **20:** 845-866

Ort DR (2001) When There Is Too Much Light. Plant Physiology **125:** 29-32

Ort DR, Merchant SS, Alric J, Barkan A, Blankenship RE, Bock R, Croce R, Hanson MR, Hibberd JM, Long SP, Moore TA, Moroney J, Niyogi KK, Parry MAJ, Peralta-Yahya PP, Prince RC, Redding KE, Spalding MH, van Wijk KJ, Vermaas WFJ, von Caemmerer S, Weber APM, Yeates TO, Yuan JS, Zhu XG (2015) Redesigning photosynthesis to sustainably meet global food and bioenergy demand. Proceedings of the National Academy of Sciences **112:** 8529-8536

Ort DR, Zhu X, Melis A (2011) Optimizing antenna size to maximize photosynthetic efficiency. Plant Physiology **155:** 79-85

Osborne BA, Raven JA (1986) Light absorption by plants and its implications for photosynthesis. Biological Reviews **61:** 1-60

Paltineanu IC, Starr JL (1997) Real-time soil water dynamics using multisensor capacitance probes: laboratory calibration. Soil Science Society of America Journal **61:** 1576-1585

Pettigrew WT, Hesketh JD, Peters DB, Woolley JT (1989) Characterization of canopy photosynthesis of chlorophyll-deficient soybean isolines. Crop Science **29:** 315-330

Polle JEW, Kanakagiri SD, Melis A (2003) Tla1, a DNA insertional transformant of the green alga *Chlamydomonas reinhardtii* with a truncated light-harvesting chlorophyll antenna size. Planta **217:** 49-59

Ray DK, Mueller ND, West PC, Foley JA (2013) Yield trends are insufficient to double global crop production by 2050. PLoS ONE **8:** e66428

Ritchie R (2006) Consistent sets of spectrophotometric chlorophyll equations for acetone, methanol and ethanol solvents. Photosynthesis Research **89:** 27-41

Salvagiotti F, Cassman KG, Specht JE, Walters DT, Weiss A, Dobermann A (2008) Nitrogen uptake, fixation and response to fertilizer N in soybeans: A review. Field Crops Research **108:** 1-13

Sands P (1995) Modelling canopy production. I. Optimal distribution of photosynthetic resources. Functional Plant Biology **22:** 593-601

Schieving F, Pons TL, Werger MJA, Hirose T (1992) The vertical distribution of nitrogen and photosynthetic activity at different plant densities in *Carex acutiformis*. Plant and Soil **142:** 9-17

Sharkey TD, Bernacchi CJ, Farquhar GD, Singsaas EL (2007) Fitting photosynthetic carbon dioxide response curves for C_3 leaves. Plant Cell & Environment **30:** 1035-1040

Slattery R, VanLoocke A, Bernacchi C, Zhu X, Ort D (2017) Photosynthesis, light use efficiency, and yield of reduced-chlorophyll soybean mutants in field conditions. Frontiers in Plant Science **8:** 549

Slattery RA, Grennan AK, Sivaguru M, Sozzani R, Ort DR (2016) Light sheet microscopy reveals more gradual light attenuation in light-green versus dark-green soybean leaves. Journal of Experimental Botany **67:** 4697-4709

Slattery RA, Ort DR (2016) Photosynthetic energy conversion efficiency: setting a baseline for gauging future improvements in important food and biofuel crops. Plant Physiology **168:** 383-392

Song Q, Wang Y, Qu M, Ort DR, Zhu X (Accepted) The impact of modifying antenna size of photosystem II on canopy photosynthetic efficiency. Plant Cell and Environment

Spinrad RW, Brown JF (1986) Relative real refractive index of marine microorganisms: a technique for flow cytometric estimation. Applied Optics **25:** 1930-1934

Syvertsen JP, Lloyd J, McConchie C, Kriedemann PE, Farquhar GD (1995) On the relationship between leaf anatomy and CO_2 diffusion through the mesophyll of hypostomatous leaves. Plant Cell & Environment **18:** 149-157

Telfer A, Pascal A, Gall A (2008) Carotenoids in Photosynthesis. *In* G Britton, S Liaaen-Jensen, H Pfander, eds, Carotenoids: Volume 4: Natural Functions. Birkhäuser Basel, Basel, pp 265-308

Terashima I, Saeki T (1983) Light environment within a leaf I. Optical properties of paradermal sections of camellia leaves with special reference to differences in the optical properties of palisade and spongy tissues. Plant and Cell Physiology **24:** 1493-1501

1184 **Vass I, Cser K** (2009) Janus-faced charge recombinations in photosystem II photoinhibition. Trends in
1185 Plant Science **14:** 200-205
1186 **Woolley JT** (1971) Reflectance and transmittance of light by leaves. Plant Physiology **47:** 656-662
1187 **Xu D, Chen X, Zhang L, Wang R, Hesketh J** (1994) Leaf photosynthesis and chlorophyll fluorescence in a
1188 chlorophyll-deficient soybean mutant. Photosynthetica **29:** 103-112
1189 **Yin X, Lantinga EA, Schapendonk AHCM, Zhong X** (2003) Some quantitative relationships between leaf
1190 area index and canopy nitrogen content and distribution. Annals of Botany **91:** 893-903
1191 **Zhu X-G, de Sturler E, Long SP** (2007) Optimizing the distribution of resources between enzymes of
1192 carbon metabolism can dramatically increase photosynthetic rate: a numerical simulation using
1193 an evolutionary algorithm. Plant Physiology **145:** 513-526
1194 **Zhu X-G, Long SP, Ort DR** (2008) What is the maximum efficiency with which photosynthesis can convert
1195 solar energy into biomass? Current Opinion in Biotechnology **19:** 153-159

1196

Parsed Citations

Ainsworth EA, Rogers A, Leakey ADB, Heady LE, Gibon Y, Stitt M, Schurr U (2007) Does elevated atmospheric [CO2] alter diurnal C uptake and the balance of C and N metabolites in growing and fully expanded soybean leaves? Journal of Experimental Botany 58: 579-591

Pubmed: Author and Title
CrossRef: Author and Title
Google Scholar: Author Only Title Only Author and Title

Anten NPR (1997) Modelling canopy photosynthesis using parameters determined from simple non-destructive measurements. Ecological Research 12: 77

Pubmed: Author and Title
CrossRef: Author and Title
Google Scholar: Author Only Title Only Author and Title

Anten NPR, Schieving F, Werger MJA (1995) Patterns of light and nitrogen distribution in relation to whole canopy carbon gain in C3 and C4 mono- and dicotyledonous species. Oecologia 101: 504-513

Pubmed: Author and Title
CrossRef: Author and Title
Google Scholar: Author Only Title Only Author and Title

Archontoulis SV, Vos J, Yin X, Bastiaans L, Danalatos NG, Struik PC (2011) Temporal dynamics of light and nitrogen vertical distributions in canopies of sunflower, kenaf and cynara. Field Crops Research 122: 186-198

Pubmed: Author and Title
CrossRef: Author and Title
Google Scholar: Author Only Title Only Author and Title

ASTM (2012) Standard Tables for Reference Solar Spectral Irradiances: Direct Normal and Hemispherical on 37° Tilted Surface. In, West Conshohocken, PA

Pubmed: Author and Title
CrossRef: Author and Title
Google Scholar: Author Only Title Only Author and Title

Bagley J, Rosenthal DM, Ruiz-Vera UM, Siebers MH, Kumar P, Ort DR, Bernacchi C (2015) The influence of photosynthetic acclimation to rising CO2 and warmer temperatures on leaf and canopy photosynthesis models. Global Biogeochemical Cycles 29: 194-206

Pubmed: Author and Title
CrossRef: Author and Title
Google Scholar: Author Only Title Only Author and Title

Baker NR (2008) Chlorophyll fluorescence: a probe of photosynthesis in vivo. Annual Review of Plant Biology 59: 89-113

Pubmed: Author and Title
CrossRef: Author and Title
Google Scholar: Author Only Title Only Author and Title

Baldocchi DD, Wilson KB, Gu L (2002) How the environment, canopy structure and canopy physiological functioning influence carbon, water and energy fluxes of a temperate broad-leaved deciduous forest- an assessment with the biophysical model CANOAK. Tree Physiology 22: 1065-1077

Pubmed: Author and Title
CrossRef: Author and Title
Google Scholar: Author Only Title Only Author and Title

Bernacchi CJ, Pimentel C, Long SP (2003) In vivo temperature response functions of parameters required to model RuBP-limited photosynthesis. Plant, Cell & Environment 26: 1419-1430

Pubmed: Author and Title
CrossRef: Author and Title
Google Scholar: Author Only Title Only Author and Title

Bernacchi CJ, Portis AR, Nakano H, von Caemmerer S, Long SP (2002) Temperature response of mesophyll conductance. Implications for the determination of Rubisco enzyme kinetics and for limitations to photosynthesis in vivo. Plant Physiology 130: 1992-1998

Pubmed: Author and Title
CrossRef: Author and Title
Google Scholar: Author Only Title Only Author and Title

Bernacchi CJ, Singsaas EL, Pimentel C, Portis AR, Long SP (2001) Improved temperature response functions for models of Rubisco-limited photosynthesis. Plant Cell & Environment 24: 253-259

Pubmed: Author and Title
CrossRef: Author and Title
Google Scholar: Author Only Title Only Author and Title

Campbell BW, Mani D, Curtin SJ, Slattery RA, Michno J-M, Ort DR, Schaus PJ, Palmer RG, Orf JH, Stupar RM (2015) Identical substitutions in magnesium chelatase paralogs result in chlorophyll-deficient soybean mutants. G3: Genes|Genomes|Genetics 5: 123-131

Pubmed: Author and Title
CrossRef: Author and Title

Google Scholar: Author Only Title Only Author and Title

Campbell G, Norman J (1998) Introduction to environmental biophysics. Springer Verlag
Pubmed: Author and Title
CrossRef: Author and Title
Google Scholar: Author Only Title Only Author and Title

De Pury D, Farquhar GD (1997) Simple scaling of photosynthesis from leaves to canopies without the errors of big-leaf models. Plant Cell & Environment 20: 537-557
Pubmed: Author and Title
CrossRef: Author and Title
Google Scholar: Author Only Title Only Author and Title

Del Pozo A, Dennett MD (1999) Analysis of the distribution of light, leaf nitrogen, and photosynthesis within the canopy of Vicia faba L. at two contrasting plant densities. Australian Journal of Agricultural Research 50: 183-190
Pubmed: Author and Title
CrossRef: Author and Title
Google Scholar: Author Only Title Only Author and Title

Dornhoff GM, Shibles R (1976) Leaf morphology and anatomy in relation to CO2-exchange rate of soybean leaves. Crop Science 16: 377-381
Pubmed: Author and Title
CrossRef: Author and Title
Google Scholar: Author Only Title Only Author and Title

Dreccer MF, van Oijen M, Schapendonk AHCM, Pot CS, Rabbinge R (2000) Dynamics of vertical leaf nitrogen distribution in a vegetative wheat canopy. Impact on canopy photosynthesis. Annals of Botany 86: 821-831
Pubmed: Author and Title
CrossRef: Author and Title
Google Scholar: Author Only Title Only Author and Title

Drewry DT, Kumar P, Long S, Bernacchi C, Liang XZ, Sivapalan M (2010a) Ecohydrological responses of dense canopies to environmental variability: 1. Interplay between vertical structure and photosynthetic pathway. Journal of Geophysical Research: Biogeosciences 115: G04022
Pubmed: Author and Title
CrossRef: Author and Title
Google Scholar: Author Only Title Only Author and Title

Drewry DT, Kumar P, Long S, Bernacchi C, Liang XZ, Sivapalan MCG (2010b) Ecohydrological responses of dense canopies to environmental variability: 2. Role of acclimation under elevated CO2. Journal of Geophysical Research: Biogeosciences 115: G04023
Pubmed: Author and Title
CrossRef: Author and Title
Google Scholar: Author Only Title Only Author and Title

Drewry DT, Kumar P, Long SP (2014) Simultaneous improvement in productivity, water use, and albedo through crop structural modification. Global Change Biology 20: 1955-1967
Pubmed: Author and Title
CrossRef: Author and Title
Google Scholar: Author Only Title Only Author and Title

Evans JR, Poorter H (2001) Photosynthetic acclimation of plants to growth irradiance: the relative importance of specific leaf area and nitrogen partitioning in maximizing carbon gain. Plant, Cell & Environment 24: 755-767
Pubmed: Author and Title
CrossRef: Author and Title
Google Scholar: Author Only Title Only Author and Title

Evans JR, Seemann JR (1989) The allocation of protein nitrogen in the photosynthetic apparatus: costs, consequences, and control. Photosynthesis: 183-205
Pubmed: Author and Title
CrossRef: Author and Title
Google Scholar: Author Only Title Only Author and Title

Evans JR, von Caemmerer S (1996) Carbon dioxide diffusion inside leaves. Plant Physiology 110: 339-346
Pubmed: Author and Title
CrossRef: Author and Title
Google Scholar: Author Only Title Only Author and Title

Farquhar GD, Sharkey TD (1982) Stomatal conductance and photosynthesis. Annual Review of Plant Physiology 33: 317-345
Pubmed: Author and Title
CrossRef: Author and Title
Google Scholar: Author Only Title Only Author and Title

Field C (1983) Allocating leaf nitrogen for the maximization of carbon gain: leaf age as a control on the allocation program. Oecologia 56: 341-347
Pubmed: Author and Title
CrossRef: Author and Title

Google Scholar: Author Only Title Only Author and Title

Flexas J, Ortuño MF, Ribas-Carbo M, Diaz-Espejo A, Flórez-Sarasa ID, Medrano H (2007) Mesophyll conductance to CO2 in Arabidopsis thaliana. New Phytologist 175: 501-511
Pubmed: Author and Title
CrossRef: Author and Title
Google Scholar: Author Only Title Only Author and Title

Foyer CH, Shigeoka S (2011) Understanding oxidative stress and antioxidant functions to enhance photosynthesis. Plant Physiology 155: 93-100
Pubmed: Author and Title
CrossRef: Author and Title
Google Scholar: Author Only Title Only Author and Title

González-Bayán R, Kinsman EA, Quesada V, Vera A, Robles P, Ponce MR, Pyke KA, Micol JL (2006) Mutations in the RETICULATA gene dramatically alter internal architecture but have little effect on overall organ shape in Arabidopsis leaves. Journal of Experimental Botany 57: 3019-3031
Pubmed: Author and Title
CrossRef: Author and Title
Google Scholar: Author Only Title Only Author and Title

Goudriaan J (1977) Crop micrometeorology: a simulation study. Pudoc, Wageningen
Pubmed: Author and Title
CrossRef: Author and Title
Google Scholar: Author Only Title Only Author and Title

Gu J, Zhou Z, Li Z, Chen Y, Wang Z, Zhang H (2017a) Rice (Oryza sativa L.) with reduced chlorophyll content exhibit higher photosynthetic rate and efficiency, improved canopy light distribution, and greater yields than normally pigmented plants. Field Crops Research 200: 58-70
Pubmed: Author and Title
CrossRef: Author and Title
Google Scholar: Author Only Title Only Author and Title

Gu J, Zhou Z, Li Z, Chen Y, Wang Z, Zhang H, Yang J (2017b) Photosynthetic properties and potentials for improvement of photosynthesis in pale green leaf rice under high light conditions. Frontiers in Plant Science 8
Pubmed: Author and Title
CrossRef: Author and Title
Google Scholar: Author Only Title Only Author and Title

Gutschick V (1984a) Photosynthesis model for C3 leaves incorporating CO2 transport, radiation propagation, and biochemistry. 1. Kinetics and their parametrization. Photosynthetica 18: 549-568
Pubmed: Author and Title
CrossRef: Author and Title
Google Scholar: Author Only Title Only Author and Title

Gutschick V (1984b) Photosynthesis model for C3 leaves incorporating CO2 transport, radiation propagation, and biochemistry. 2. Ecological and agricultural utility. Photosynthetica 18: 569-595
Pubmed: Author and Title
CrossRef: Author and Title
Google Scholar: Author Only Title Only Author and Title

Gutschick V (1988) Optimization of specific leaf mass, internal CO2 concentration, and chlorophyll content in crop canopies. Plant Physiology and Biochemistry 26: 525-537
Pubmed: Author and Title
CrossRef: Author and Title
Google Scholar: Author Only Title Only Author and Title

Hikosaka K, Niinemets U, Anten NP (2016) Canopy photosynthesis: from basics to applications. Springer
Pubmed: Author and Title
CrossRef: Author and Title
Google Scholar: Author Only Title Only Author and Title

Hikosaka K, Terashima I (1995) A model of the acclimation of photosynthesis in the leaves of C3 plants to sun and shade with respect to nitrogen use. Plant, Cell & Environment 18: 605-618
Pubmed: Author and Title
CrossRef: Author and Title
Google Scholar: Author Only Title Only Author and Title

Kirst H, Gabilly ST, Niyogi KK, Lemaux PG, Melis A (2017) Photosynthetic antenna engineering to improve crop yields. Planta: 1-12
Pubmed: Author and Title
CrossRef: Author and Title
Google Scholar: Author Only Title Only Author and Title

Kirst H, Garcia-Cerdan JG, Zurbriggen A, Ruehle T, Melis A (2012) Truncated photosystem chlorophyll antenna size in the green microalga Chlamydomonas reinhardtii upon deletion of the TLA3-CpSRP43 gene. Plant Physiology 160: 2251-2260

Pubmed: Author and Title
CrossRef: Author and Title
Google Scholar: Author Only Title Only Author and Title

Koester RP, Skoneczka JA, Cary TR, Diers BW, Ainsworth EA (2016) Historical gains in soybean (Glycine max Merr.) seed yield are driven by linear increases in light interception, energy conversion, and partitioning efficiencies. Journal of Experimental Botany 65: 3311-3321
Pubmed: Author and Title
CrossRef: Author and Title
Google Scholar: Author Only Title Only Author and Title

Kromdijk J, Long SP (2016) One crop breeding cycle from starvation? How engineering crop photosynthesis for rising CO2 and temperature could be one important route to alleviation. Proceedings of the Royal Society B: Biological Sciences 283
Pubmed: Author and Title
CrossRef: Author and Title
Google Scholar: Author Only Title Only Author and Title

Kuhlbrandt W, Wang DN, Fujiyoshi Y (1994) Atomic model of plant light-harvesting complex by electron crystallography. Nature 367: 614-621
Pubmed: Author and Title
CrossRef: Author and Title
Google Scholar: Author Only Title Only Author and Title

Lai C-T, Katul G, Oren R, Ellsworth D, Schäfer K (2000) Modeling CO2 and water vapor turbulent flux distributions within a forest canopy. Journal of Geophysical Research: Atmospheres 105: 26333-26351
Pubmed: Author and Title
CrossRef: Author and Title
Google Scholar: Author Only Title Only Author and Title

Laisk A (1982) Correspondence of photosynthetic system to environmental conditions. In N AA, ed, Fiziologiya fotosinteza. Nauka, Moscow, pp 221-234
Pubmed: Author and Title
CrossRef: Author and Title
Google Scholar: Author Only Title Only Author and Title

Lange BM, Ghassemian M (2003) Genome organization in Arabidopsis thaliana: a survey for genes involved in isoprenoid and chlorophyll metabolism. Plant Molecular Biology 51: 925-948
Pubmed: Author and Title
CrossRef: Author and Title
Google Scholar: Author Only Title Only Author and Title

Lee C-G (1999) Calculation of light penetration depth in photobioreactors. Biotechnology and Bioprocess Engineering 4: 78-81
Pubmed: Author and Title
CrossRef: Author and Title
Google Scholar: Author Only Title Only Author and Title

Leuning R, Kelliher FM, De Pury DGG, Schulze ED (1995) Leaf nitrogen, photosynthesis, conductance and transpiration: scaling from leaves to canopies. Plant Cell & Environment 18: 1183-1200
Pubmed: Author and Title
CrossRef: Author and Title
Google Scholar: Author Only Title Only Author and Title

Lindgren LO, Stålberg KG, Höglund A-S (2003) Seed-specific overexpression of an endogenous arabidopsis phytoene synthase gene results in delayed germination and increased levels of carotenoids, chlorophyll, and abscisic acid. Plant Physiology 132: 779-785
Pubmed: Author and Title
CrossRef: Author and Title
Google Scholar: Author Only Title Only Author and Title

Long SP, Marshall-Colon A, Zhu X-G (2015) Meeting the global food demand of the future by engineering crop photosynthesis and yield potential. Cell 161: 56-66
Pubmed: Author and Title
CrossRef: Author and Title
Google Scholar: Author Only Title Only Author and Title

Long SP, Zhu X-G, Naidu SL, Ort DR (2006) Can improvement in photosynthesis increase crop yields? Plant Cell & Environment 29: 315-330
Pubmed: Author and Title
CrossRef: Author and Title
Google Scholar: Author Only Title Only Author and Title

Melis A (1999) Photosystem-II damage and repair cycle in chloroplasts: what modulates the rate of photodamage in vivo? Trends in Plant Science 4: 130-135
Pubmed: Author and Title
CrossRef: Author and Title
Google Scholar: Author Only Title Only Author and Title

Mitra M, Melis A (2008) Optical properties of microalgae for enhanced biofuels production. Optics Express 16: 21807-21820
Pubmed: Author and Title
CrossRef: Author and Title
Google Scholar: Author Only Title Only Author and Title

Moreau D, Allard V, Gaju O, Le Gouis J, Foulkes MJ, Martre P (2012) Acclimation of leaf nitrogen to vertical light gradient at anthesis in wheat is a whole-plant process that scales with the size of the canopy. Plant Physiology 160: 1479-1490
Pubmed: Author and Title
CrossRef: Author and Title
Google Scholar: Author Only Title Only Author and Title

Netto AT, Campostrini E, Oliveira JGd, Bressan-Smith RE (2005) Photosynthetic pigments, nitrogen, chlorophyll a fluorescence and SPAD-502 readings in coffee leaves. Scientia Horticulturae 104: 199-209
Pubmed: Author and Title
CrossRef: Author and Title
Google Scholar: Author Only Title Only Author and Title

Niinemets Ü (2007) Photosynthesis and resource distribution through plant canopies. Plant, Cell & Environment 30: 1052-1071
Pubmed: Author and Title
CrossRef: Author and Title
Google Scholar: Author Only Title Only Author and Title

Niinemets Ü, Keenan TF, Hallik L (2015) A worldwide analysis of within-canopy variations in leaf structural, chemical and physiological traits across plant functional types. New Phytologist 205: 973-993
Pubmed: Author and Title
CrossRef: Author and Title
Google Scholar: Author Only Title Only Author and Title

Niinemets Ü, Tenhunen JD (1997) A model separating leaf structural and physiological effects on carbon gain along light gradients for the shade-tolerant species Acer saccharum. Plant, Cell & Environment 20: 845-866
Pubmed: Author and Title
CrossRef: Author and Title
Google Scholar: Author Only Title Only Author and Title

Ort DR (2001) When There Is Too Much Light. Plant Physiology 125: 29-32
Pubmed: Author and Title
CrossRef: Author and Title
Google Scholar: Author Only Title Only Author and Title

Ort DR, Merchant SS, Alric J, Barkan A, Blankenship RE, Bock R, Croce R, Hanson MR, Hibberd JM, Long SP, Moore TA, Moroney J, Niyogi KK, Parry MAJ, Peralta-Yahya PP, Prince RC, Redding KE, Spalding MH, van Wijk KJ, Vermaas WFJ, von Caemmerer S, Weber APM, Yeates TO, Yuan JS, Zhu XG (2015) Redesigning photosynthesis to sustainably meet global food and bioenergy demand. Proceedings of the National Academy of Sciences 112: 8529-8536
Pubmed: Author and Title
CrossRef: Author and Title
Google Scholar: Author Only Title Only Author and Title

Ort DR, Zhu X, Melis A (2011) Optimizing antenna size to maximize photosynthetic efficiency. Plant Physiology 155: 79-85
Pubmed: Author and Title
CrossRef: Author and Title
Google Scholar: Author Only Title Only Author and Title

Osborne BA, Raven JA (1986) Light absorption by plants and its implications for photosynthesis. Biological Reviews 61: 1-60
Pubmed: Author and Title
CrossRef: Author and Title
Google Scholar: Author Only Title Only Author and Title

Paltineanu IC, Starr JL (1997) Real-time soil water dynamics using multisensor capacitance probes: laboratory calibration. Soil Science Society of America Journal 61: 1576-1585
Pubmed: Author and Title
CrossRef: Author and Title
Google Scholar: Author Only Title Only Author and Title

Pettigrew WT, Hesketh JD, Peters DB, Woolley JT (1989) Characterization of canopy photosynthesis of chlorophyll-deficient soybean isolines. Crop Science 29: 315-330
Pubmed: Author and Title
CrossRef: Author and Title
Google Scholar: Author Only Title Only Author and Title

Polle JEW, Kanakagiri SD, Melis A (2003) Tla1, a DNA insertional transformant of the green alga Chlamydomonas reinhardtii with a truncated light-harvesting chlorophyll antenna size. Planta 217: 49-59
Pubmed: Author and Title
CrossRef: Author and Title
Google Scholar: Author Only Title Only Author and Title

Ray DK, Mueller ND, West PC, Foley JA (2013) Yield trends are insufficient to double global crop production by 2050. PLoS ONE 8:

e66428
Pubmed: Author and Title
CrossRef: Author and Title
Google Scholar: Author Only Title Only Author and Title

Ritchie R (2006) Consistent sets of spectrophotometric chlorophyll equations for acetone, methanol and ethanol solvents. Photosynthesis Research 89: 27-41
Pubmed: Author and Title
CrossRef: Author and Title
Google Scholar: Author Only Title Only Author and Title

Salvagiotti F, Cassman KG, Specht JE, Walters DT, Weiss A, Dobermann A (2008) Nitrogen uptake, fixation and response to fertilizer N in soybeans: A review. Field Crops Research 108: 1-13
Pubmed: Author and Title
CrossRef: Author and Title
Google Scholar: Author Only Title Only Author and Title

Sands P (1995) Modelling canopy production. I. Optimal distribution of photosynthetic resources. Functional Plant Biology 22: 593-601
Pubmed: Author and Title
CrossRef: Author and Title
Google Scholar: Author Only Title Only Author and Title

Schieving F, Pons TL, Werger MJA, Hirose T (1992) The vertical distribution of nitrogen and photosynthetic activity at different plant densities in Carex acutiformis. Plant and Soil 142: 9-17
Pubmed: Author and Title
CrossRef: Author and Title
Google Scholar: Author Only Title Only Author and Title

Sharkey TD, Bernacchi CJ, Farquhar GD, Singsaas EL (2007) Fitting photosynthetic carbon dioxide response curves for C3 leaves. Plant Cell & Environment 30: 1035-1040
Pubmed: Author and Title
CrossRef: Author and Title
Google Scholar: Author Only Title Only Author and Title

Slattery R, VanLoocke A, Bernacchi C, Zhu X, Ort D (2017) Photosynthesis, light use efficiency, and yield of reduced-chlorophyll soybean mutants in field conditions. Frontiers in Plant Science 8: 549
Pubmed: Author and Title
CrossRef: Author and Title
Google Scholar: Author Only Title Only Author and Title

Slattery RA, Grennan AK, Sivaguru M, Sozzani R, Ort DR (2016) Light sheet microscopy reveals more gradual light attenuation in light-green versus dark-green soybean leaves. Journal of Experimental Botany 67: 4697-4709
Pubmed: Author and Title
CrossRef: Author and Title
Google Scholar: Author Only Title Only Author and Title

Slattery RA, Ort DR (2016) Photosynthetic energy conversion efficiency: setting a baseline for gauging future improvements in important food and biofuel crops. Plant Physiology 168: 383-392
Pubmed: Author and Title
CrossRef: Author and Title
Google Scholar: Author Only Title Only Author and Title

Song Q, Wang Y, Qu M, Ort DR, Zhu X (Accepted) The impact of modifying antenna size of photosystem II on canopy photosynthetic efficiency. Plant Cell and Environment

Spinrad RW, Brown JF (1986) Relative real refractive index of marine microorganisms: a technique for flow cytometric estimation. Applied Optics 25: 1930-1934
Pubmed: Author and Title
CrossRef: Author and Title
Google Scholar: Author Only Title Only Author and Title

Syvertsen JP, Lloyd J, McConchie C, Kriedemann PE, Farquhar GD (1995) On the relationship between leaf anatomy and CO2 diffusion through the mesophyll of hypostomatous leaves. Plant Cell & Environment 18: 149-157
Pubmed: Author and Title
CrossRef: Author and Title
Google Scholar: Author Only Title Only Author and Title

Telfer A, Pascal A, Gall A (2008) Carotenoids in Photosynthesis. In G Britton, S Liaaen-Jensen, H Pfander, eds, Carotenoids: Volume 4: Natural Functions. Birkhäuser Basel, Basel, pp 265-308
Pubmed: Author and Title
CrossRef: Author and Title
Google Scholar: Author Only Title Only Author and Title

Terashima I, Saeki T (1983) Light environment within a leaf I. Optical properties of paradermal sections of camellia leaves with special reference to differences in the optical properties of palisade and spongy tissues. Plant and Cell Physiology 24: 1493-1501

Pubmed: Author and Title
CrossRef: Author and Title
Google Scholar: Author Only Title Only Author and Title

Vass I, Cser K (2009) Janus-faced charge recombinations in photosystem II photoinhibition. Trends in Plant Science 14: 200-205
Pubmed: Author and Title
CrossRef: Author and Title
Google Scholar: Author Only Title Only Author and Title

Woolley JT (1971) Reflectance and transmittance of light by leaves. Plant Physiology 47: 656-662
Pubmed: Author and Title
CrossRef: Author and Title
Google Scholar: Author Only Title Only Author and Title

Xu D, Chen X, Zhang L, Wang R, Hesketh J (1994) Leaf photosynthesis and chlorophyll fluorescence in a chlorophyll-deficient soybean mutant. Photosynthetica 29: 103-112
Pubmed: Author and Title
CrossRef: Author and Title
Google Scholar: Author Only Title Only Author and Title

Yin X, Lantinga EA, Schapendonk AHCM, Zhong X (2003) Some quantitative relationships between leaf area index and canopy nitrogen content and distribution. Annals of Botany 91: 893-903
Pubmed: Author and Title
CrossRef: Author and Title
Google Scholar: Author Only Title Only Author and Title

Zhu X-G, de Sturler E, Long SP (2007) Optimizing the distribution of resources between enzymes of carbon metabolism can dramatically increase photosynthetic rate: a numerical simulation using an evolutionary algorithm. Plant Physiology 145: 513-526
Pubmed: Author and Title
CrossRef: Author and Title
Google Scholar: Author Only Title Only Author and Title

Zhu X-G, Long SP, Ort DR (2008) What is the maximum efficiency with which photosynthesis can convert solar energy into biomass? Current Opinion in Biotechnology 19: 153-159
Pubmed: Author and Title
CrossRef: Author and Title
Google Scholar: Author Only Title Only Author and Title